

# A Deep Learning Based Resource Allocator for Communication Systems with Dynamic User Utility Demands

Pourya Behmandpoor, Mark Eisen, Panagiotis Patrinos, Marc Moonen

**Abstract**—Deep learning (DL) based resource allocation (RA) has recently gained significant attention due to its performance efficiency. However, most related studies assume an ideal case where the number of users and their utility demands, e.g., data rate constraints, are fixed, and the designed DL-based RA scheme exploits a policy trained only for these fixed parameters. Consequently, computationally complex policy retraining is required whenever these parameters change. In this paper, we introduce a DL-based resource allocator (ALCOR) that allows users to adjust their utility demands freely, such as based on their application layer requirements. ALCOR employs deep neural networks (DNNs) as the policy in a time-sharing problem. The underlying optimization algorithm iteratively optimizes the on-off status of users to satisfy their utility demands in expectation. The policy performs unconstrained RA (URA)—RA without considering user utility demands—among active users to maximize the sum utility (SU) at each time instant. Depending on the chosen URA scheme, ALCOR can perform RA in either a centralized or distributed scenario. Derived convergence analyses provide guarantees for ALCOR’s convergence, and numerical experiments corroborate its effectiveness.

**Index Terms**—Resource allocation, deep learning, dynamic data rate constraints, utility function, centralized and distributed

## I. INTRODUCTION

Resource allocation (RA) in communication systems has been an active research topic for decades [1]–[4], resulting in the development of various RA schemes. Since the underlying optimization problem is nonconvex and possibly large-scale, conventional RA schemes typically exhibit slow convergence in large communication systems. Moreover, these schemes cannot be easily extended either to consider longer time horizons, e.g., to perform RA for an average of utilities over time, or to address the vast interconnection of users

This research work was carried out at the ESAT Laboratory of KU Leuven, in the frame of Research Project FWO nr. G0C0623N ‘User-centric distributed signal processing algorithms for next generation cell-free massive MIMO based wireless communication networks’. The work is also supported by the Research Foundation Flanders (FWO) postdoctoral grant 12Y7622N and research projects G081222N, G033822N, and G0A0920N; Research Council KU Leuven C1 project No. C14/24/103; European Union’s Horizon 2020 research and innovation programme under the Marie Skłodowska-Curie grant agreement No. 953348. The scientific responsibility is assumed by its authors. Pourya Behmandpoor, Panagiotis Patrinos, and Marc Moonen are with KU Leuven University, Department of Electrical Engineering (ESAT), STADIUS Center for Dynamical Systems, Signal Processing and Data Analytics (e-mail: pourya.behmandpoor, marc.moonen, panos.patrinos@esat.kuleuven.be). Mark Eisen is with Johns Hopkins University, Applied Physics Laboratory (e-mail: mark.eisen@ieee.org).

taking their various mutual effects into account. These limitations motivate recent advancements in deep learning (DL)-based RA, where a policy, such as a deep neural network (DNN), is typically dedicated to translating dynamic parameters of the communication system, e.g., channel coefficients, into optimal resources, e.g., the optimal transmit power for each user [5], [6].

Existing DL-based RA schemes in the literature incorporate various training strategies. The policies are either trained in a supervised manner [7], where RA solutions are available as labels, or in an unsupervised manner [8]–[11], where a utility function, e.g., sum data rate of users, is considered the global reward function. Alternatively, policies can serve as decision-makers that monitor the state space, e.g., the set of channel coefficients, and choose actions within the action space, e.g., different transmit power levels. Such policies can be trained using reinforcement learning (RL) principles [12]–[15]. The mentioned training strategies are mostly model-based; they assume a model for the reward, and the trainer optimizes the policy parameters using the calculated gradient of this model. An alternative training approach is model-free, where the gradient is approximated by various methods, such as policy gradient (REINFORCE [16]) or zeroth-order optimization, by measuring reward values [17]–[19]. This training can also be performed in real-time while the communication system is operating. Through real-time reward measurement, this approach can capture the full behavior of the system, including nonidealities such as nonlinearities in the modulator and demodulator or antenna setup, which are not typically captured by model-based approaches due to simplifications.

In the inference step, existing DL-based RA schemes are employed in either a centralized or a distributed manner. In a centralized approach, a server is responsible for conducting the RA by gathering necessary information from all users and employing a centralized policy for RA [12], [13], [15], [19]. In the distributed variants, each user conducts RA by employing their local policies, possibly with message-passing between users to share necessary information. In this scenario, the policies can be either identical among the users [13], [15] or different [12]. Distributed RA can also employ graph neural networks (GNN) [20] to enhance RA robustness against scalability [19], [21]–[24]. Furthermore, the training step is classified as either centralized or distributed [12], [13], [15], [19], [25], [26].

RA can be categorized into *unconstrained* RA and *constrained* RA. In unconstrained RA, a global reward function

is optimized with minimal constraints, such as simple box constraints that can be managed by a simple projection through an appropriate output activation function. However, this approach cannot address more complex constraints, such as user demands. Specifically, the RA is unable to allocate more resources to users with higher demands. A common workaround is optimizing the weighted sum utilities as the global reward function [11], [27], where the weights reflect the users' utility demands. Conversely, in constrained RA, a global reward function is optimized while meeting more complex utility demands, such as data rate constraints. During policy training, these constraints are typically managed either by including a penalization term in the reward function [8], or by using the primal-dual optimization method, which directly addresses constrained optimization problems [18], [19], [22], [23].

To the best of our knowledge, the RA schemes in the literature utilize policies, such as DNNs, which are trained for a fixed set of utility demands and a fixed number of users. However, in practice, the number of active users is subject to change, and it is more efficient if the RA scheme allows users to have dynamic utility demands based on their real-time tasks. Policy retraining becomes necessary if any of the mentioned fixed parameters change. This limitation undermines the applicability of existing DL-based RA schemes, as policy retraining is a computationally complex task, leading to delays in real-time exploitation. One possible workaround is to incorporate dynamic utility demands, along with all other dynamic components of the communication system, into the policy input. In this case, the policy would be trained for different utility demands as well. However, generalizing the problem with a moderate amount of resources, such as the number of layers and neurons in DNN policies, is not practically feasible. This has already been experimentally validated in [11] and our simulations. In works such as [22], constraints are made dynamic, meaning they are allowed to deviate from the initial utility demands. However, this deviation is determined by the RA scheme itself and is not freely chosen by the users. Furthermore, in [28], the concepts of transfer learning [29] are used to fine-tune only a part of the policy, such as the last few layers, to reduce the computational complexity of retraining. However, this fine-tuning is useful only when the modified RA scheme is similar enough to the initial RA scheme, which is not necessarily the case. In the same view, meta-learning [30]–[33] aims to warm start a policy by finding its initial parameters such that the policy can effectively generalize to new tasks, e.g., new sets of utility demands, after being fine-tuned using a few data points from the new tasks. Meta-learning assumes a distribution of tasks that share common high-level structures. It also requires computationally demanding training, and its capability to generalize to new tasks highly depends on the similarity of tasks, which is not always obvious in RA with dynamic utility demands.

*Objective:* In this paper<sup>1</sup>, the objective is to propose a DL-based RA scheme that can adapt, on average over time, to dynamic user utility demands. The novelty of this work lies in the fact that, unlike existing DL-based RA schemes, the adap-

tation to new sets of user utility demands does not require any retraining of the involved policies, thereby conserving computational resources and improving speed.

*Contributions:* The contributions are listed as follows:

- (i) A RA scheme is proposed, which involves time-sharing and DL-based RA among the users. At each time instant, the proposed RA scheme selects a subset of users to be activated and performs DL-based RA among these activated users to maximize their sum utility (SU). The proposed time-sharing algorithm is an optimization algorithm that iteratively controls the on-off status of users to guarantee their utility demands in expectation.
- (ii) Convergence analyses are provided for the proposed RA scheme under standard assumptions, deriving a convergence rate of  $\mathcal{O}(1/\sqrt{k})$ , with  $k$  representing the iteration counter in the considered time-sharing algorithm.
- (iii) Rigorous numerical experiments are conducted to assess the performance of the proposed RA scheme and its distributed variant against various benchmarks.

## II. SYSTEM MODEL

We consider  $N$  users (links) each equipped with a transmitter and a receiver. The direct channel between the transmitter and receiver of user  $i$  is denoted by  $h_{ii}$ , while the interference channel between the transmitter of user  $j$  and the receiver of user  $i$  is denoted by  $h_{ij}$ . All the channel coefficients define the full channel matrix  $\mathbf{H} \in \mathbb{C}^{N \times N}$  with  $h_{ij}$  as its element in the  $i$ th row and  $j$ th column.

For the RA, we consider a central deep neural network (DNN) as the policy defined by

$$\phi(\mathbf{S}, \boldsymbol{\theta}) : \mathbb{R}^s \times \Theta \rightarrow \mathbb{R}^N \quad (1)$$

with input  $\mathbf{S}$  and policy parameter  $\boldsymbol{\theta} \in \Theta \subset \mathbb{R}^n$ . Here  $\mathbf{S}$  is a random variable incorporating global or local measurements of agents, which vary over time and is a function of parameters such as the global channel  $\mathbf{H}$  and the agents' state. Examples of elements in  $\mathbf{S}$  could include channel coefficients, packet queue length awaiting transmission, or received interference power from neighbors (cf. Section IV for more details). The policy parameter  $\boldsymbol{\theta}$  may contain DNN weights and biases, to be optimized during training. The policy output specifies (ideally to be optimal) resources such as transmit power, frequency band, timeslot, beamformer angle, etc. of all  $N$  users. The policy described in (1) is designed for centralized RA, where a single server manages RA. Distributed extensions will be discussed in Remark III.2.

## III. PROPOSED METHOD

### A. Problem statement

Before formally stating the problem, consider the user selection vector  $\boldsymbol{\xi}$  defined as follows:

**Definition III.1** (user selection vector (USV)  $\boldsymbol{\xi}$ ). *Define the USV as  $\boldsymbol{\xi} = (\xi_1, \dots, \xi_N) \in \Omega^\xi := \{0, 1\}^N$ . The elements  $\xi_i$  are drawn from a Bernoulli distribution with mean:*

$$\kappa_i := \mathbb{E}\{\xi_i\} \in [0, 1], \quad \forall i \in [N]. \quad (2)$$

<sup>1</sup>This paper is an extension of the work presented in [34].

By the USV, user  $i$  is selected to be active if  $\xi_i = 1$ , otherwise it is switched off. Moreover, the USV distribution is denoted by  $\mathcal{D}^\xi(\boldsymbol{\kappa})$  with  $\boldsymbol{\kappa} := (\kappa_1, \dots, \kappa_N) \in \mathbb{R}^N$ .

Note that according to (2), the probability that user  $i$  is activated is  $\kappa_i$ , based on the assumed Bernoulli distribution. After defining the USV  $\boldsymbol{\xi}$ , we are interested in the following problems:

#### Time-sharing problem:

Find the optimal probabilities  $\boldsymbol{\kappa} = (\kappa_1, \dots, \kappa_N) \in [0, 1]^N$  for activating users at each time instant, based on  $\boldsymbol{\xi} \sim \mathcal{D}^\xi(\boldsymbol{\kappa})$ , such that:

- The utility demands of all users are satisfied in expectation (on average over time);

#### Resource allocation problem:

At each time instant, allocate resources among the users such that:

- The SU is maximized among active users for a given  $\boldsymbol{\xi} \in \Omega^\xi$  and  $\mathbf{H}$ .

After optimizing the probabilities  $\boldsymbol{\kappa}$ , at each time instant, a random instance of the USV  $\boldsymbol{\xi}$  defined in Definition III.1 is drawn. Then, according to  $\boldsymbol{\xi}$ , some users are activated while others are deactivated. Subsequently, a URA is performed among the active users.

Before addressing the mentioned problems, the basic assumptions made throughout the paper are as follows:

#### Assumption I (basic assumptions).

- The dynamic parameters of the communication system, e.g., the channel  $\mathbf{H}$ , are ergodic stochastic variables, with possibly unknown distributions;
- The utility demands  $\mathbf{u}^{\min}$  are changing slower than the dynamic parameters of the communication system, and are assumed to be constant in time windows.

It is remarked that in Assumption I, utility demands  $\mathbf{u}^{\min}$  are not assumed to be fixed, which is a restrictive assumption in the literature that we aim to relax. Moreover, Assumption I(i) regarding the dynamic parameters of the communication system is a standard assumption in the literature [13], [15], [23], [24]. Assumption I(ii) is a mild assumption in practice since utility demands  $\mathbf{u}^{\min}$  mostly reflect the demands originating from the application layer, e.g., following a task scheduling scheme based on currently running tasks. These demands are slower in nature, typically changing at a rate of seconds or more, compared to the channel dynamics in wireless communication systems, which typically change at a rate of milliseconds in fast-fading scenarios (cf. Section III-D for further explanation).

#### B. Unconstrained resource allocation (URA)

To address the DL-based URA for each  $\boldsymbol{\xi}$  and  $\mathbf{H}$ , the RA policy  $\phi$  defined in (1) is trained using the following unconstrained optimization:

$$\underset{\boldsymbol{\theta} \in \mathbb{R}^n}{\text{maximize}} \sum_{i \in [N]} \mathbb{E}_{\mathbf{H} \sim \mathcal{D}^H, \boldsymbol{\kappa} \sim \mathcal{D}^\kappa, \boldsymbol{\xi} \sim \mathcal{D}^\xi(\boldsymbol{\kappa})} [U_i^\theta(\mathbf{H}_\xi)], \quad (3)$$

$$\text{where } U_i^\theta(\mathbf{H}_\xi) := U_i(\mathbf{H}_\xi, \phi(\mathbf{S}_\xi, \boldsymbol{\theta})),$$

with  $U_i(\mathbf{H}_\xi, \phi(\mathbf{S}_\xi, \boldsymbol{\theta}))$  as the utility of user  $i$ , e.g., its data rate, which depends on the communication channel  $\mathbf{H}_\xi$  and the resources, e.g., user transmit powers, allocated to all users by  $\phi(\mathbf{S}_\xi, \boldsymbol{\theta})$ . Here,  $\mathbf{H}_\xi$  denotes the global channel for the subset of active users, which equals the channel matrix  $\mathbf{H}$  with distribution  $\mathcal{D}^H$  except for rows and columns corresponding to the zero elements of  $\boldsymbol{\xi}$  (deactivated users), which are set to zero. Similarly,  $\mathbf{S}_\xi$  contains measurements of the active users, and  $\boldsymbol{\kappa} := (\kappa_1, \dots, \kappa_N)$  with a uniform distribution  $\mathcal{D}^\kappa$  in  $[0, 1]^N$ . For simplicity, the policy input  $\mathbf{S}_\xi$  is assumed to be a function of only the channel  $\mathbf{H}$ , so is  $U_i^\theta$ .

In problem (3), the policy parameter is optimized to maximize the SU of users in expectation, serving as a global utility function. This problem can be addressed using first-order stochastic gradient descent (SGD) over batches of random samples. This leads to the following iterations with an initial value  $\boldsymbol{\theta}^0$  and an iteration counter  $\ell \in [L-1]$  with  $L > 0$ :

$$\boldsymbol{\theta}^{\ell+1} = \boldsymbol{\theta}^\ell + \frac{\gamma^\ell}{B} \sum_{i \in [N]} \sum_{j=1}^B \nabla_{\boldsymbol{\theta}} U_i^{\theta^\ell}(\mathbf{H}_\xi^{\ell,j}). \quad (4)$$

In (4), sample averaging is performed over batches of size  $B$  with channels  $\mathbf{H}_\xi^{\ell,j}$  and probabilities  $\boldsymbol{\kappa}^{\ell,j}$  where  $\boldsymbol{\xi}^{\ell,j} \sim \mathcal{D}^\xi(\boldsymbol{\kappa}^{\ell,j})$ . Here, the superscript  $\{\ell, j\}$  indicates the  $j$ th sample in the batch taken at iteration  $\ell$ . The step size is also denoted by  $\gamma^\ell$ . The capability of policy  $\phi$  to generalize the URA problem for all possible  $\mathbf{H}$ ,  $\boldsymbol{\xi}$ , and  $\boldsymbol{\kappa}$  heavily depends on the policy resources, such as the number of layers and perceptrons in each layer in the case of a DNN policy. Due to the limited memory and computational capacities, as well as the nonconvex nature of the problem, generalization is often suboptimal in practice.

During the inference stage, the trained policy is utilized to perform URA among active users at each time instant as follows:

$$r_i := [\phi(\mathbf{S}_\xi, \boldsymbol{\theta}^L)]_i \quad \text{if } \xi_i = 1, \quad (5)$$

$$r_i := 0 \quad \text{if } \xi_i = 0,$$

where  $[\cdot]_i$  indicates the  $i$ th element of the vector and  $r_i$  defines the allocated resource for user  $i$ .

#### C. Time-sharing

After training the policy  $\phi(\cdot, \boldsymbol{\theta}^L)$  for URA, we proceed to formulate the time-sharing problem as defined in Section III-A. To do so, we first define the following function  $F: \mathbb{R}^N \rightarrow \mathbb{R}^N$

$$F(\boldsymbol{\lambda}) := \mathbb{E}_{\mathbf{H}, \boldsymbol{\xi} \sim \mathcal{D}^\xi(\boldsymbol{\kappa})} [\hat{F}(\mathbf{H}_\xi)], \quad (6)$$

$$\text{where } \hat{F}(\mathbf{H}_\xi) := \mathbf{u}^{\min} - \mathbf{U}^{\boldsymbol{\theta}^L}(\mathbf{H}_\xi),$$

$$\kappa_i = (1 + \lambda_i) / \max_\ell \{1 + \lambda_\ell\},$$

with  $\boldsymbol{\lambda} \in \mathbb{R}_+^N$ ,  $\boldsymbol{\kappa}$  defined in Definition III.1, and  $\mathbf{U}^{\boldsymbol{\theta}^L} := (U_1^{\boldsymbol{\theta}^L}, \dots, U_N^{\boldsymbol{\theta}^L})$ .

In (6), we aim to solve the following problem:

$$\text{find } \boldsymbol{\lambda} \in \mathbb{R}_+^N \text{ such that } F(\boldsymbol{\lambda}) \leq \mathbf{0}, \quad (7)$$

where  $\mathbf{0} \in \mathbb{R}^N$  is a vector of all zeros and  $\leq$  is an element-wise operator. The equality  $[F(\boldsymbol{\lambda})]_i = 0$  indicates that the expected utility of user  $i$ ,  $\mathbb{E}_{\mathbf{H}, \boldsymbol{\xi} \sim \mathcal{D}^\xi(\boldsymbol{\kappa})} [U_i^{\boldsymbol{\theta}^L}(\mathbf{H}_\xi)]$ , is equal



**Algorithm 1** ALCOR

**Input** utility demands  $\mathbf{u}^{\min}$ , step sizes  $\gamma > 0$ ,  $\alpha_k \in (0, 1)$ ,  
batchsize  $B > 0$

**Initialize**  $\bar{\lambda}^{-1} = \bar{\lambda}^0 \in \mathbb{R}^N$ ,  $\mathbf{h}^0 \in \mathbb{R}^N$ ,  $\boldsymbol{\kappa}^0 \in \mathbb{R}^N$

**Repeat**  $k = 0, 1, \dots, K - 1$

- 1: Sample a batch of  $\boldsymbol{\xi}^{k,j} \sim \mathcal{D}^\xi(\boldsymbol{\kappa}^k)$  with  $j \in [B]$
- 2: Perform URA (5) and form the average  $\hat{F}(\mathbb{H}_\xi^k)$  in (8)
- 3:  $\mathbf{h}^{k+1} := \bar{\lambda}^k + \gamma \hat{F}(\mathbb{H}_\xi^k) + (1 - \alpha_k)(\mathbf{h}^k - \bar{\lambda}^{k-1} - \gamma \hat{F}(\mathbb{H}_\xi^k))$
- 4:  $\boldsymbol{\lambda}^{k+1} = \max\{\mathbf{0}, \mathbf{h}^{k+1}\}$
- 5: Sample a batch of  $\bar{\boldsymbol{\xi}}^{k,j} \sim \mathcal{D}^\xi(\boldsymbol{\kappa}^k)$  with  $j \in [B]$
- 6: Perform URA (5) and form the average  $\hat{F}(\bar{\mathbb{H}}_\xi^k)$  in (8)
- 7:  $\bar{\lambda}^{k+1} = \bar{\lambda}^k - \alpha_k(\mathbf{h}^{k+1} - \boldsymbol{\lambda}^{k+1} - \gamma \hat{F}(\bar{\mathbb{H}}_\xi^k))$
- 8:  $\kappa_i^{k+1} = (1 + \lambda_i^{k+1}) / \max_\ell \{1 + \lambda_\ell^{k+1}\}$ ,  $\forall i \in [N]$

to its utility demand  $u_i^{\min}$ , while  $[F(\boldsymbol{\lambda})]_i < 0$  indicates that the expected utility of user  $i$  is greater than its demand. To guarantee inequality (7), we propose using  $\boldsymbol{\lambda}$  to calculate the probabilities  $\kappa_i$ . This choice is motivated by the fact that  $\kappa_i$  remains nonzero for any choice of  $\boldsymbol{\lambda}$  in (7), maintaining higher utility for the corresponding user, and yet, whenever required,  $\kappa_i$  can become arbitrarily small by choosing large  $\lambda_j$  by other users  $j$ . Thus, the coupling between users, which is due to interference in the communication system, can be captured by this definition of  $\kappa_i$ .

To estimate the expectation in (6), we define the following sample average:

$$\hat{F}(\mathbb{H}_\xi^k) := \frac{1}{B} \sum_{j=1}^B \hat{F}(\mathbf{H}_\xi^{k,j}), \quad (8)$$

where  $\mathbb{H}_\xi^k$  refers to the batch of samples, defined as  $\mathbb{H}_\xi^k := \{\mathbf{H}_\xi^{k,1}, \dots, \mathbf{H}_\xi^{k,B}\}$  and  $\mathbf{H}_\xi^{k,j}$  represents the  $j$ th sample in a batch of size  $B$ , taken at iteration  $k$  with USV  $\boldsymbol{\xi}^k$ . The algorithm for finding  $\boldsymbol{\lambda}$  in (7) is outlined in the next subsection.

#### D. Algorithm

The proposed algorithm for the time-sharing problem (7) is summarized in Algorithm 1, which can be easily implemented using the mappings defined in (6) and (8). At each iteration  $k$ , in step 1, the algorithm activates a subset of users according to the USV instance  $\boldsymbol{\xi}^{k,j} \sim \mathcal{D}^\xi(\boldsymbol{\kappa}^k)$ , which depends on the most updated probabilities  $\boldsymbol{\kappa}^k := (\kappa_1^k, \dots, \kappa_N^k)$ . Then, in step 2, URA is performed among the activated users to maximize their SU. This procedure is repeated  $B$  times for each  $j \in [B]$  to form a batch, allowing the calculation of the sample average (8). Following step 3, the current parameter  $\boldsymbol{\lambda}^k$  is updated using either a fixed step size  $\alpha_k = \alpha$  or a diminishing step size  $\alpha_k = \alpha_0 / \sqrt{1 + \tilde{\alpha}k}$  with some  $\alpha_0, \tilde{\alpha} > 0$ . Step 4 ensures the nonnegativity of updates, i.e.,  $\boldsymbol{\lambda}^k \in \mathbb{R}_+^N$ . The same steps are repeated for a new batch of samples  $\bar{\boldsymbol{\xi}}^{k,j} \sim \mathcal{D}^\xi(\boldsymbol{\kappa}^k)$ , based on the same probabilities  $\boldsymbol{\kappa}^k$ , in step 5. Updates are performed following steps 6 and 7 with a new batch of channel samples  $\bar{\mathbb{H}}_\xi^k := \{\bar{\mathbf{H}}_\xi^{k,1}, \dots, \bar{\mathbf{H}}_\xi^{k,B}\}$ . At the end, in step 8, the probabilities  $\boldsymbol{\kappa}^k$  are updated using the updated nonnegative parameters  $\boldsymbol{\lambda}^{k+1}$ . During the iterations, the utility demands are assumed

to remain fixed within a time window of length  $T$ , which is sufficiently long to allow the algorithm to meet the utility demands on average over time, i.e.,  $K \ll T$ . Moreover, once utility demands are updated, the algorithm restarts with a new input  $\mathbf{u}^{\min}$ .

It is noted that the two-step updates (steps 4 and 7) can be seen as extragradient-like updates [35], where during one iteration, the algorithm first generates an intermediate iterate  $\mathbf{h}^{k+1}$  from a base iterate  $\bar{\lambda}^k$  and then completes the update by taking a step from the base iterate using the intermediate iterate. The time-sharing problem (7) can also be implemented by a simpler algorithm where a batch of samples  $\boldsymbol{\xi}^{k,j} \sim \mathcal{D}^\xi(\boldsymbol{\kappa}^k)$  is employed, followed by URA among the activated users and calculating the average in (8). Then the parameter  $\boldsymbol{\lambda}^k$  can be updated by  $\boldsymbol{\lambda}^{k+1} = \max\{\mathbf{0}, \boldsymbol{\lambda}^k + \alpha_k \hat{F}(\mathbb{H}_\xi^k)\}$  at each iteration  $k$ . This update rule guarantees an increase in  $\lambda_i$ , and subsequently the probability  $\kappa_i$ , whenever the average utility of user  $i$  is below its demand  $u_i^{\min}$ . However, there is no convergence guarantee for this simpler update rule in the optimization literature. Convergence analysis for Algorithm 1 is provided in the Appendix, where the time-sharing problem (7) is cast as an inclusion problem under the category of nonmonotone variational inequalities [36].

**Remark III.2** (distributed ALCOR). Due to the definition of the mapping  $\hat{F}$  in (6), Algorithm 1 can be readily extended to a distributed variant, where each user has an individual policy  $\phi_i$  to perform distributed URA [12], [13], [15]. In this case, the policies are trained according to (3), with  $U_i^\theta(\mathbf{H}_\xi) := U_i(\mathbf{H}_\xi, \phi(\mathcal{S}_\xi, \boldsymbol{\theta}))$ . The utility  $U_i^\theta$  depends on all individual policies  $\phi(\mathcal{S}_\xi, \boldsymbol{\theta}) := (\phi_1(\mathcal{S}_{\xi,1}, \boldsymbol{\theta}_1), \dots, \phi_N(\mathcal{S}_{\xi,N}, \boldsymbol{\theta}_N))$ , which are based on individual local measurements  $\mathcal{S}_{\xi,i}$  and individual policy parameters  $\boldsymbol{\theta}_i$  possibly without consensus, i.e.,  $\boldsymbol{\theta}_i \neq \boldsymbol{\theta}_j$  for  $i \neq j$ . Moreover, URA in (5) can be performed with  $r_i = \phi_i(\mathcal{S}_{\xi,i}, \boldsymbol{\theta}_i^L)$  if  $\xi_i = 1$ , and  $r_i = 0$  otherwise. It is noteworthy that in distributed ALCOR, although the utility  $U_i^\theta$  depends on all individual policies, user  $i$  only requires its own utility. Each user  $i$  locally executes Algorithm 1 with local variables  $\lambda_i^k, \bar{\lambda}_i^k, h_i^k$ , and  $\kappa_i^k$ , utilizing local estimates  $[\hat{F}(\mathbb{H}_\xi^k)]_i$  and  $[\hat{F}(\bar{\mathbb{H}}_\xi^k)]_i$ . Additionally, to update  $\kappa_i^k$  in step 8, each user needs the normalization term  $\max_\ell \{1 + \lambda_\ell^{k+1}\}$ , which can be obtained by exchanging scalar values  $\lambda_\ell^{k+1}$  among users via message-passing. This distributed variant is also considered in the numerical experiments (see Section IV for further details).  $\square$

**Remark III.3** (agnostic to URA methods). The proposed RA scheme can employ policies as a black box for URA. These policies can be centralized or distributed and can be trained and utilized by various DL methods, such as RL, GNN, etc. [8], [13], [21]. In the distributed variant, the individual policies  $\phi_i$  may be different, i.e.,  $\boldsymbol{\theta}_i \neq \boldsymbol{\theta}_j$  for  $i \neq j$  [12], or there may be a consensus among them, i.e.,  $\boldsymbol{\theta}_i = \boldsymbol{\theta}_j$  for  $i \neq j$  [13], [15], depending on the employed distributed URA scheme.  $\square$

The scalability of the proposed method, the maximum number of users that ALCOR can accommodate for RA, and the communication overhead in the distributed variant depend on

the employed URA method. Since ALCOR is agnostic to URA methods, suitable methods can be selected based on the communication system of interest. Furthermore, ALCOR is limited to scenarios that can be formulated by (6) and (7). Specifically, ALCOR can address RA problems where increasing  $\kappa_i$ , the probability of user  $i$  being activated, leads to an increase in the user's utility and consequently satisfies its demand.

#### E. Convergence study

The convergence rate of [Algorithm 1](#) is provided in the following theorem. The formal convergence statement and its proof are presented in [Appendix B](#).

**Theorem III.4** (informal). *Algorithm 1 converges with a rate of  $\mathcal{O}(1/\sqrt{k})$ , where  $k$  denotes the iteration number.*

This theorem states that for a sufficiently large time window length  $T$ , ALCOR converges to an optimal time-sharing policy within the scope of the time window, and users can operate while meeting their current utility demands.

### IV. NUMERICAL EXPERIMENTS

In this section, we evaluate the proposed RA scheme through numerical experiments across various communication scenarios. We address the power allocation problem where user utilities are defined as data rates. Specifically, the resources are the transmit powers  $\mathbf{r} = \mathbf{p} = (p_1, \dots, p_N) \in [0, p^{max}]^N$ , constrained by a maximum  $p^{max}$ , and utilities are data rates, where  $U_i = R_i$  and

$$R_i(\mathbf{H}, \mathbf{p}) := \log_2 \left( 1 + \frac{|h_{ii}|^2 p_i}{\sigma_n^2 + \sum_{j \neq i} |h_{ij}|^2 p_j} \right), \quad (9)$$

with  $\sigma_n^2$  as the power of independent and identically distributed (IID) additive white Gaussian noise at the receivers. Two centralized and distributed URA schemes, adopted from [\[8\]](#), [\[15\]](#), are employed for policy training and performing URA among the activated users.

**Centralized policy:** A fully connected DNN is considered as the URA policy, following the structure outlined in [\[8\]](#). Specifically, it consists of 4 layers with the number of neurons set to  $\{400, 400, 200, 20\}$ , unless specified otherwise. The policy input is the full channel matrix  $\mathbf{H}$ , denoted as  $\mathbf{S} = \mathbf{H}$  in (1), and the output is the continuous transmit power of all users  $\mathbf{p}$ . With the considered policy, URA can be performed for a maximum number of 20 users, although the number of active users per time instant may be fewer. The activation function of hidden layers is the rectified linear unit (relu), while for the output layer, the *sigmoid* function is considered to ensure compliance with the transmit power box constraint. Batch normalization is also applied during training in all layers except the output layer. The policy structure is the same throughout the simulations unless specified otherwise.

**Distributed policy:** A fully connected deep neural network (DNN) is considered as the URA policy, comprising 4 layers with the number of neurons set to  $\{41, 100, 50, 1\}$ . As shown in [\[15\]](#), all users utilize the same DNN, i.e.,  $\phi_1 = \dots = \phi_N$ .

Each user collects local measurements to feed into its local policy and adjusts its continuous transmit power based on the policy output. The activation functions are consistent with the centralized case, and batch normalization is also employed. Define the following sets

$$\begin{aligned} \mathcal{I}_i^t &:= \{j \in [N], j \neq i \mid |h_{ij}^t|^2 p_j^t > \eta \sigma^2\}, \\ \mathcal{O}_i^t &:= \{j \in [N], j \neq i \mid |h_{ji}^t|^2 p_i^t > \eta \sigma^2\}, \end{aligned}$$

for user  $i$  at time  $t$ . Here,  $\mathcal{I}_i^t$  represents the set of users at time  $t$  causing interference to user  $i$ , where the interference power exceeds the threshold  $\eta \sigma^2$ . Conversely,  $\mathcal{O}_i^t$  represents the set of users at time  $t$  receiving interference from user  $i$  exceeding the same threshold. In the simulations, the maximum cardinality of these sets is limited to 5 by selecting 5 most affected users in  $\mathcal{O}_i^t$  and 5 most affecting users in  $\mathcal{I}_i^t$ , and the parameter  $\eta$  is fixed at 1. The local measurements of user  $i$  at time  $t$ , used as input for its policy  $\phi_i$ , are obtained from [\[15\]](#) and are included here for completeness:

- Transmit power  $p_i^{t-1}$  and data rate  $R_i^{t-1}$ ;
- Direct channels  $|h_{ii}^t|^2$  and  $|h_{ii}^{t-1}|^2$ ;
- Received interference power from all users in two time instants:  $\sum_{j=1, j \neq i}^N |h_{ij}^t|^2 p_j^{t-1} + \sigma^2$ ,  $\sum_{j=1, j \neq i}^N |h_{ij}^{t-1}|^2 p_j^{t-2} + \sigma^2$ ;
- Received interference power from interfering neighbors in the set  $\mathcal{I}_i$  in two timeslots:  $\{|h_{ij}^t|^2 p_j^{t-1} \mid j \in \mathcal{I}_i^{t-1}\}$ ,  $\{|h_{ij}^{t-1}|^2 p_j^{t-2} \mid j \in \mathcal{I}_i^{t-2}\}$ ;
- Data rate of the interfering neighbors:  $\{R_j^{t-1} \mid j \in \mathcal{I}_i^{t-1}\}$ ,  $\{R_j^{t-2} \mid j \in \mathcal{I}_i^{t-2}\}$ ;
- Normalized transmitted interference power to affected neighbors in the set  $\mathcal{O}_i$  as  $\{|h_{ji}^{t'}|^2 p_i^{t'} (\sum_{i=1, i \neq j}^N |h_{ji}^{t-1}|^2 p_i^{t-1} + \sigma^2)^{-1} \mid j \in \mathcal{O}_i^{t'}\}$ , where  $t'$  is the last time when user  $i$  was active;
- Direct channel of interfered neighbors:  $\{|h_{jj}^{t-1}|^2 \mid j \in \mathcal{O}_i^{t'}\}$ ;
- Data rate of interfered neighbors:  $\{R_j^{t-1} \mid j \in \mathcal{O}_i^{t'}\}$ .

The input set  $\mathbf{S}_i$  for each user  $i$  comprises 41 elements, forming the local policy input. If the sets  $\mathcal{I}_i$  and  $\mathcal{O}_i$  contain fewer than 5 elements, zero-padding is applied at the respective policy input locations to ensure a fixed input size. The policy uses past measurements to accommodate channel instances that are correlated over time. However, initial simulations suggest that this correlation has negligible impact on the proposed RA scheme performance on the considered tasks. Therefore, we report the results with IID channel samples.

**Policy training:** In both centralized and distributed scenarios, policies are trained using an unsupervised approach, as discussed in [\[8\]](#), where the reward function during the training is (3). The distributions for  $\mathbf{H}$ ,  $\kappa$ , and  $\xi$  vary in different scenarios and are specified in the sequel.

#### Benchmarks:

- (i) **Fixed DNN:** A DNN is considered in the centralized scenario for each user number  $N$ , where the utility demands  $\mathbf{u}^{\text{fix}} \in \mathbb{R}^N$  are fixed and are to be satisfied in expectation. The detailed architecture of the DNNs will be mentioned

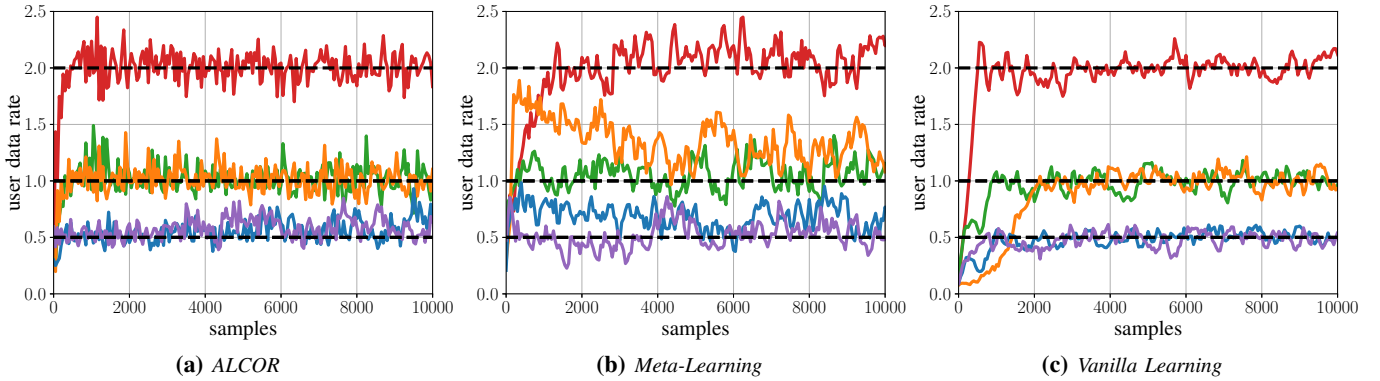


**Figure 1:** Performance comparison of different RA schemes in a 5-user centralized scenario with a similar DNN structure of  $\{25, 25, 25, 5\}$ . Each color specifies the instantaneous data rate of a user in bps/Hz over time, where the utility demands (data rate demands)  $\mathbf{u}^{\min} = (0.5, 0.5, 1, 1, 2)$  are depicted by black dashed lines. While the proposed scheme (ALCOR) does not involve any DNN retraining, meta-learning and vanilla learning (re)train the DNN using the reward function of (10). The (re)training is performed with a diminishing step size of  $\psi^*/_{1+k}$ , where  $k$  is the epoch counter and  $\psi^* \approx 0.3$  from (11). ALCOR demonstrates faster and more stable convergence.

subsequently for each  $N$ . The DNNs are trained in an unsupervised manner [8] using the reward function

$$\text{reward}(\boldsymbol{\theta}, \mathbf{u}^{\text{fix}}) = \sum_{i=1}^N \mathbb{E}_{\mathbf{H}} [U_i^{\boldsymbol{\theta}}(\mathbf{H})] - L \sum_{i=1}^N \max\{0, u_i^{\text{fix}} - \mathbb{E}_{\mathbf{H}} [U_i^{\boldsymbol{\theta}}(\mathbf{H})]\}, \quad (10)$$

where constraint violations are penalized with  $L = 100$ . During training, expectations are approximated using batches of size 1000. Note that this reward function differs from the one in [8, eq. (14)], where the DNN is forced to satisfy the utility demands for every channel instance  $\mathbf{H}$ .

- (ii) **Dynamic DNN:** A DNN with the structure of  $\{25 + 5, 200, 100, 5\}$  is considered in the centralized scenario for  $N = 5$  users with dynamic utility demands. The DNN's input consists of the full channel  $\mathbf{H}$  along with the dynamic utility demands  $\mathbf{u}^{\min}$ . The reward function remains consistent with (10). During the training,  $u_i^{\min}$  is uniformly selected from the interval  $[0, 5]$  and is updated 100 times slower than the channel.
- (iii) **WMMSE:** The conventional iterative URA scheme WMMSE [4] is considered for assessing the trained policies in URA and as a black box URA scheme used within the proposed RA scheme.
- (iv) **GP:** The iterative geometric programming (GP) RA scheme [3] is also considered, which is able to satisfy the utility demands for each channel instance. When comparing with this method, only channel instances feasible for the GP optimization problem are considered in the comparison.
- (v) **Meta-learning:** The meta-learning approach presented by [31] is considered in a 5-user centralized scenario, where a DNN with the structure  $\{25, 25, 25, 5\}$  is warm-started such that it can quickly adapt to a new set of utility demands after a single update. Particularly, the model is trained to

$$\begin{aligned} & \text{maximize } \mathbb{E}_{\mathbf{u}^{\min}} [\text{reward}(\boldsymbol{\theta}^+, \mathbf{u}^{\min})] \\ & \boldsymbol{\theta} \in \mathbb{R}^n, \psi > 0 \end{aligned} \quad (11)$$

subject to  $\boldsymbol{\theta}^+ := \boldsymbol{\theta} + \psi \nabla_{\boldsymbol{\theta}} \text{reward}(\boldsymbol{\theta}, \mathbf{u}^{\min})$ , where reward is defined in (10),  $\mathbf{u}^{\min}$  is uniformly sam-

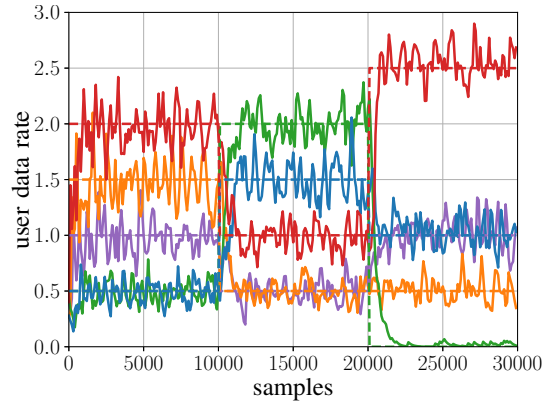


**Figure 2:** Satisfying utility demands (on average) in a 5-user centralized scenario using ALCOR. Three time windows with different utility demands,  $\mathbf{u}^{\min}$ , are shown. Each solid line represents the instantaneous data rate of a user in bps/Hz over time, and the dashed lines represent the dynamic utility demands of the corresponding colors.

pled from the interval  $[0, 2.5]^N$ , and the expectation in reward is approximated using exponential averaging with a decay factor of 0.7 over batches of size 1000 during training and 50 during inference. The optimization parameters  $\boldsymbol{\theta}$  and  $\psi$  in (11) are optimized following the procedure outlined in [31] with step sizes of  $10^{-4}$  and  $5 \times 10^{-6}$ , respectively.

In the simulations, the step sizes of Algorithm 1 are set as constants, with  $\alpha_k = 0.9$  and suitable values of  $\gamma$  ranging from 1 to 10, depending on the specific experiment. The batch size is set  $B = 25$ , unless specified otherwise. In the rest of this section, two different channel scenarios are considered for performance evaluation.

#### A. Circularly symmetric channel

In this section, the channel coefficients are assumed to follow a circularly symmetric complex normal distribution, i.e.

$\kappa$	cntr. (divs.)	cntr. (non-divs.)	dist. (divs.)	dist. (non-divs.)	WMMSE
0.25	5.88	5.63	5.82	5.45	5.88
0.5	6.38	6.30	6.31	6.09	6.8
0.75	6.56	6.56	6.52	6.35	7.29
1	6.71	6.72	6.66	6.62	7.72

**Table I:** URA performance comparison between DL-based policies and WMMSE for  $N = 20$  users. SR is reported in bps/Hz. Centralized and distributed policies are considered with diverse training (where  $\kappa$  is randomly sampled during training) and non-diverse training (where  $\kappa = 1$  remains constant during training) strategies. These policies are only responsible for unconstrained RA and cannot satisfy user utility demands.

$N$	ALCOR (cntr.)	ALCOR (dist.)	fixed DNN	GP
10	5.41	4.37	6.82	3.86
20	6.56	6.37	6.73	3.81
50	6.67	5.95	6.16	4.73

**Table II:** Comparison of various RA schemes with different numbers of users and utility demands. SR is reported in bps/Hz. All utility demands are satisfied without violation. The utility demands are zero except for the following users:  $N = 10$ :  $\mathbf{u}_{1:10}^{\min} = 0.25$ ,  $N = 20$ :  $\mathbf{u}_{1:12}^{\min} = 0.1$ ,  $N = 50$ :  $\mathbf{u}_{1:15}^{\min} = 0.05$ . The fixed DNNs are trained using the reward function (10) with the utility demands considered for each  $N$ .

$N$	ALCOR (cntr.)		ALCOR (dist.)		fixed DNN	
	SR	viol.%	SR	viol.%	SR	viol.%
10	3.13	0.61	3.85	0.01	6.35	37.71
20	3.97	0.00	5.35	0.00	6.58	60.45
50	6.09	1.37	4.75	2.84	6.17	64.14

**Table III:** Stricter utility demands than the ones in Table II. SR is reported in bps/Hz and violation is calculated by (12). The utility demand are zero except for the following users:  $N = 10$ :  $\mathbf{u}_{1:10}^{\min} = 0.1$  except  $u_5^{\min} = 0.6, u_7^{\min} = 0.8, u_9^{\min} = 1$ ,  $N = 20$ :  $\mathbf{u}_{1:10}^{\min} = 0.1$  except  $u_5^{\min} = 0.4, u_7^{\min} = 0.6, u_{12}^{\min} = 0.2, u_{19}^{\min} = 0.8$ ,  $N = 50$ :  $\mathbf{u}_{20:30}^{\min} = 0.3$ . The fixed DNNs are trained with the utility demands reported in Table II.

$h_{ij} \sim \mathcal{CN}(0, 1)$ , and the SNR is set to 15 dB.

In the first experiment, the performance of the proposed RA scheme in addressing dynamic utility demands is compared with *vanilla learning* and the meta-learning approach. In both approaches, the RA policy is retrained in an unsupervised manner using the reward function in (10) for the new utility demands. In vanilla learning, the policy is initially randomized, while in meta-learning, the policy is initially warm-started by the optimization in (11), with a single update for  $\theta^+$ , similar to the simulations conducted in [31]. It is noted that meta-learning requires the Hessian of the reward function, making it computationally demanding. According to Fig. 1, following Algorithm 1, ALCOR adapts to user utility demands with simpler updates, i.e., without retraining the policy. Its adaptation is faster and more stable compared to the other approaches. Although in the considered meta-learning approach, the objective is to find a good adaptation strategy with a single update, i.e., optimal  $\theta$  and  $\psi$  in (11), it is evident that meta-learning cannot adapt to utility demands with a single update and requires more updates. This inability for fast adaptation can be attributed to the fact that RA tasks share limited high-level structures, necessitating more iterations for fine-tuning the policy. Therefore, in our experiments, meta-learning adaptation is continued with a diminishing step size

to study the performance of RA with additional updates. Compared to vanilla learning, meta-learning is faster in satisfying utility demands due to its educated initialization.

ALCOR's adaptivity is also illustrated in Fig. 2. In a scenario with 5 users, the utility demands values are set as  $\mathbf{u}^{\min} = (0.5, 0.5, 1, 1.5, 2)$ ,  $\mathbf{u}^{\min} = (2, 1.5, 0.5, 0.5, 1)$ , and  $\mathbf{u}^{\min} = (0, 1, 1, 0.5, 2.5)$  in bps/Hz over three consecutive time windows. The figure clearly shows that the proposed RA scheme can accurately adapt to the changing utility demands and meet them on average within a few iterations after each utility demand update.

In the next experiment, we assess the performance of the centralized and distributed policies, which are trained using (3), in URA as compared to WMMSE. Two training strategies are employed: 1) *Diverse training*: During training,  $\kappa$  is randomly and uniformly chosen from the set  $\kappa \in \{0.2 \times \mathbf{1}, 0.5 \times \mathbf{1}, \mathbf{1}\}$ , where  $\mathbf{1}$  is a vector of all ones. At each time instant, each user is independently switched on with a probability of  $\kappa_i$  during the training. 2) *Non-diverse training*: During training,  $\kappa = \mathbf{1}$ , i.e., all users are always switched on.

The performance of the policies in URA is presented in Table I. Based on Table I, diverse training results in a slightly better generalization compared to non-diverse training. The performance of the policies in URA is also comparable to WMMSE, i.e., the policies maintain good performance in URA while making URA faster. The same performance is evident in [8]. As diverse and non-diverse training strategies are comparable in performance, for the remaining experiments, we employ non-diverse training, which is the standard training method in the URA literature.

In the next experiment, the proposed RA scheme is compared against the GP method and the DNNs trained using the reward function (10) for fixed utility demands (fixed DNNs). As the GP method requires a feasible RA problem at each time instant, only channels feasible for the corresponding utility demands are considered. The feasibility is determined using the procedure outlined in [37]. Centralized and distributed policies are trained using both feasible and infeasible training samples with performance assessed under varying numbers of users in the communication system. The fixed DNNs have the following structures  $\{100, 400, 200, 10\}$ ,  $\{400, 400, 200, 20\}$ , and  $\{2500, 400, 400, 50\}$  for 10, 20, and 50 users, respectively. Table II reports the achieved sum rate (SR) of users while the utility demands are satisfied, on average. The user utility demands are reported in the caption where we use the notation  $u_{a:b}^{\min}$  to refer to the utility demand of users  $i \in \{a, a+1, \dots, b\}$ . The results indicate that the proposed method outperforms the GP method in terms of SR. Further-



more, although the fixed DNNs, trained for fixed utility demands, achieve the highest SR, they can only satisfy the fixed utility demands for which they were trained. A notable advantage of the proposed method is that it is not limited to feasible channel instances, unlike methods such as the one proposed in [8]. Consequently, the proposed method does not require the computationally complex feasibility check during training. The utility demand violations are not reported in Table II, as they are equal to zero for all the reported RA schemes.

In the following, ALCOR is assessed under stricter utility demands. In this scenario, the problem is infeasible for most test samples, and the GP method is unable to provide any solution. The utility demand violation is reported as:

$$\text{viol.} := \max_{i \in [N]} \{ \max\{0, u_i^{\min} - R_i\} / u_i^{\min} \} \times 100. \quad (12)$$

Additionally, the fixed DNNs are the same as those in Table II. The results are summarized in Table III. According to the results, the proposed RA scheme can accurately satisfy dynamic utility demands while maintaining a high SR. As expected, the fixed DNNs cannot meet the new set of utility demands, and they require retraining of their policies. The instantaneous user data rates and their moving averages are also plotted in Fig. 3 for the case where  $N = 20$ . It is evident that the user data rates rapidly converge to meet the demands upon any change. The values  $\lambda$  are also plotted, showing higher values for users with greater demands. This finding aligns with what is expected from (6) and (7), where higher values of  $\lambda_i$  increase the probability  $\kappa_i$  of user  $i$  being active, thereby pushing its expected utility toward higher values.

In the final experiment of this section, we report the performance of the proposed RA scheme, where WMMSE is used as a black box URA scheme, instead of a DL-based URA scheme (cf. Remark III.3). Since WMMSE is slower compared to DNNs, we conduct the test with only  $N = 5$  users. The performance is compared against a fixed DNN, which is trained for the utility demands  $\mathbf{u}^{\min,2}$  in Table IV with the structure  $\{25, 100, 50, 5\}$ . DNN dynamic, listed among the benchmarks, is also included for comparison. According to Table IV, the proposed RA algorithm, employing different black box URA schemes, achieves a high level of accuracy in meeting the demands while maintaining a high SR. It is apparent that both the fixed DNN and dynamic DNN fail to meet the dynamic utility demands, even in such a small RA problem involving only 5 users.

### B. Multi-link per cell channel

In this section, the proposed RA scheme is assessed considering a communication system consisting of 7 cells. Each cell contains a number of transmitters and receivers, with transmitters positioned at the center and receivers uniformly distributed within the cell. The minimum and maximum allowed distances between the transmitters and the receivers are set to  $r = 50$  and  $R = 500$  meters, respectively. Noise power  $\sigma_n^2$  is set to -114 dBm,  $p_{max} = 38$  dBm, and the large-scale fading component, i.e., the path loss between transmitter  $i$  and receiver  $j$  is determined by  $\alpha_{ji} = 120.9 + 37.6 \log_{10}(d_{ji})$  dB, where  $d_{ji}$  denotes the distance measured in kilometers. The small-scale fading

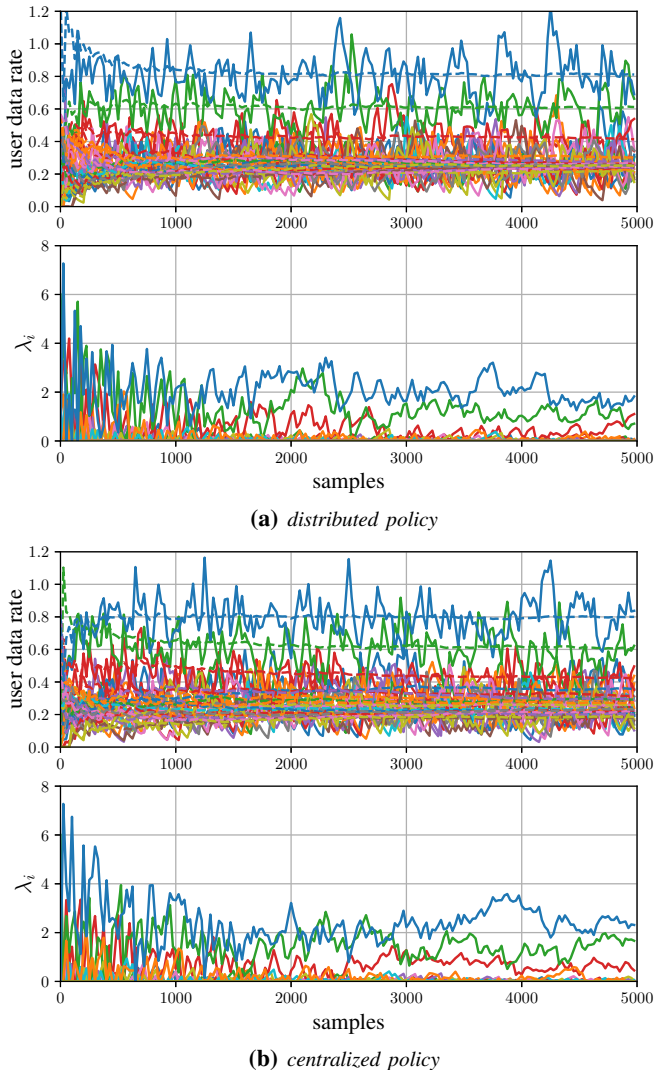


**Figure 3:** User utilities and the corresponding  $\lambda_i$ s by ALCOR for the RA scenario reported in Table III with  $N = 20$ . Each color represents the instantaneous data rate of a user in bps/Hz and the dashed lines represent the corresponding moving averages.

component follows IID circularly symmetric Gaussian distribution, i.e.,  $g_{ij} \sim \mathcal{CN}(0, 1)$ . Hence, the channel coefficients are derived as  $|h_{ij}|^2 = |g_{ij}|^2 / 10^{\alpha_{ij}/10}$ . The large-scale fading component changes 50 times slower than the small-scale fading component. Both the centralized and distributed DNNs are trained using possibly infeasible samples in the training stage. The structures of the DNNs are the same as those described in Section IV-A.

The proposed RA scheme is evaluated where utility demands are high, making the inclusion problem (7) (equivalently the RA problem) infeasible. In practical scenarios, having a method capable of continuing the RA process in such scenarios is valuable. We consider utility demands that make the problem infeasible for a system accommodating  $N = 50$  users. Fig. 4 shows that although the proposed RA scheme is unable to satisfy the utility demands in this case, the user rates are converging to values close to the corresponding utility de-



$\mathbf{u}^{\min}$	ALCOR with various black-box URA schemes						other DL-based RA schemes			
	centralized policy		distributed policy		centralized WMMSE		dynamic DNN		fixed DNN	
	SR	viol.	SR	viol.	SR	viol.	SR	viol.	SR	viol.
$\mathbf{u}^{\min,1}$	5.80	0.00	5.24	0.00	5.27	0.00	5.66	0.00	5.35	100.0
$\mathbf{u}^{\min,2}$	5.20	0.00	4.64	1.27	5.09	0.00	5.53	49.51	5.35	0.00
$\mathbf{u}^{\min,3}$	4.90	0.00	4.35	0.78	4.81	0.00	5.41	70.80	5.35	30.04

**Table IV:** Performance of ALCOR using different black box URA schemes for  $N = 5$ . SR is reported in bps/Hz and violation is calculated using (12). The considered utility demands are  $\mathbf{u}^{\min,1} = (0.5, 0.5, 0.5, 0.5, 0.5)$ ,  $\mathbf{u}^{\min,2} = (0, 1, 1.5, 2, 0)$ , and  $\mathbf{u}^{\min,3} = (0, 0, 0, 1, 3)$ . The fixed DNN is trained with the utility demand  $\mathbf{u}^{\min,2}$  using the reward function (10).

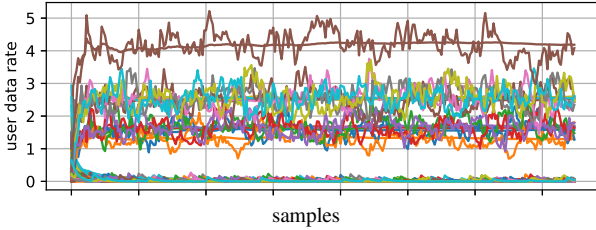


**Figure 4:** User utilities by centralized ALCOR for an infeasible RA problem with  $N = 50$ . Each color represents the instantaneous data rate of a user in bps/Hz. The utility demands are zero except for the following users:  $\mathbf{u}_{20:25}^{\min} = 2$ ,  $\mathbf{u}_{25:30}^{\min} = 3$ ,  $\mathbf{u}_{31}^{\min} = 5$ .

mands.

For the mentioned communication system in this section, ALCOR is also compared against GP and fixed DNNs and the impact of batch size on its performance is studied. The results are available in the supplementary material.

## V. CONCLUSION AND FUTURE DIRECTIONS

In this paper, a DL-based RA scheme has been proposed that utilizes DNNs as URA policies within an iterative optimization algorithm to meet dynamic user utility demands in expectation. The optimization algorithm addresses a time-sharing problem by optimizing the on-off status of users. In parallel, URA policies are responsible for performing unconstrained RA among active users at each time instant to maximize their SU. The proposed approach is agnostic to URA schemes. Consequently, depending on the employed URA policy, the proposed RA scheme can be implemented in either a centralized or distributed scenario. Convergence analyses have been provided, relying on variational inequalities, to establish convergence guarantees.

In the proposed RA scheme, users have the capability to harvest power during time-sharing. Hence, exploring the use of the proposed RA scheme for simultaneous wireless information and power transfer is an interesting future direction.

## APPENDIX A

In this Appendix, we present the notation, basic assumptions, and a lemma that are required for the convergence analysis.

### A. Notation

The distance from  $\lambda \in \mathbb{R}^N$  to a set  $\mathcal{X} \subseteq \mathbb{R}^N$  is given by  $\text{dist}(\lambda, \mathcal{X}) := \min_{v \in \mathcal{X}} \|v - \lambda\|$ . An operator  $F : \mathbb{R}^N \rightrightarrows \mathbb{R}^n$  maps each point  $\lambda \in \mathbb{R}^N$  to a set  $F\lambda \equiv F(\lambda) \subseteq \mathbb{R}^n$ . The graph of operator  $F$  is denoted by  $\text{gph } F := \{(\lambda, v) \in \mathbb{R}^N \times \mathbb{R}^n \mid v \in F\lambda\}$ . The set of zeros is defined by  $\text{zer } F := \{\lambda \in \mathbb{R}^N \mid 0 \in F\lambda\}$ . Operator  $F$  is  $\rho$ -strongly monotone with some  $\rho \geq 0$  if  $\langle v - v', \lambda - \lambda' \rangle \geq \rho \|\lambda - \lambda'\|^2$  for all  $(\lambda, v), (\lambda', v') \in \text{gph } F$ . The operator is called monotone if  $\rho = 0$ . The deviation between two distributions  $\mathcal{D}$  and  $\mathcal{D}'$  is measured using the Wasserstein-1 distance:

$$W_1(\mathcal{D}, \mathcal{D}') = \sup_{g \in \text{lip}_1} \{\mathbb{E}_{x \sim \mathcal{D}}[g(x)] - \mathbb{E}_{y \sim \mathcal{D}'}[g(y)]\}, \quad (13)$$

where  $\text{lip}_1$  denotes the set of 1-Lipschitz continuous functions  $g : \mathbb{R}^N \rightarrow \mathbb{R}^n$ .

### B. Preliminary Assumptions and Lemmas

The following assumptions are required for the convergence:

**Assumption II** (feasibility of inclusion problem (7)). *The inclusion problem (7) is feasible, namely, there exists at least one  $\lambda^* \in \mathbb{R}^N$  such that  $F(\lambda^*) \leq 0$ .*

In Algorithm 1, ALCOR utilizes a DL model within an iterative optimization algorithm. The DL model is integrated into the mapping  $F$  within the inclusion problem (7). The feasibility of the problem then depends on several factors, including the utility demands  $\mathbf{u}^{\min}$ , the capability of the DL model to generalize the URA problem, the quality of training in Section III-B, and the characteristics of the communication system, such as the quality of communication channel. Hence, the communication system requires to have mechanisms to ensure this feasibility (cf. Fig. 4 and the corresponding explanations for further details).

**Assumption III** (assumption on the expected utility). *The expected utility  $\mathbb{E}_{\mathbf{H}}[U^{\theta^L}(\mathbf{H}_{\xi})]$  is Lipschitz continuous in  $\xi$ . Namely, there is a  $\beta > 0$  such that for all  $\xi, \xi'$ :*

$$\left\| \mathbb{E}_{\mathbf{H}}[U^{\theta^L}(\mathbf{H}_{\xi})] - \mathbb{E}_{\mathbf{H}}[U^{\theta^L}(\mathbf{H}_{\xi'})] \right\| \leq \beta \|\xi - \xi'\|.$$

This assumption ensures that when the USV changes, the change in the expected utilities is bounded. This is easily verifiable for many utilities e.g., data rates where the resource is the transmit power.

To continue with the convergence analysis, we recast the problem (7) to the following inclusion problem:

$$\text{find } \lambda \in \mathbb{R}^N \text{ such that } \mathbf{0} \in T\lambda := F\lambda + A\lambda, \quad (14)$$

with  $A\lambda := \partial\varphi(\lambda)$  as the subdifferential of the indicator function  $\varphi$  defined as  $\varphi(\lambda) = 0$  if  $\lambda \in \mathbb{R}_+^N$  and  $\varphi(\lambda) = -\infty$  otherwise. The inclusion problem (14) ensures finding a variable  $\lambda$  such that  $F(\lambda) \leq \mathbf{0}$ . This is achieved under two conditions: 1)  $\mathbf{0} \in T\lambda$  with  $[F\lambda]_i = 0$  and  $[A\lambda]_i = 0$  for some  $i \in [N]$ . 2)  $\mathbf{0} \in T\lambda$  with  $[F\lambda]_i < 0$  and  $[A\lambda]_i > 0$  for some  $i \in [N]$ . The second case is possible thanks to the definition of  $\kappa_i$  allowing  $\kappa_i$  to be nonzero when  $\lambda_i = 0$ , thereby permitting  $[F\lambda]_i < 0$ . It is remarked that, by the definition of  $A$ , the case where  $\mathbf{0} \in T\lambda$  with  $[F\lambda]_i > 0$  and  $[A\lambda]_i < 0$  never occurs. The necessary assumptions on the mappings of inclusion problem (14) are as follows:

**Assumption IV** (assumptions on the mappings  $F, \hat{F}, A$ ).

(i) The mapping  $F : \mathbb{R}^N \rightarrow \mathbb{R}^N$  is Lipschitz continuous with the constant  $L_F \in [0, +\infty)$ :

$$\|F(\lambda) - F(\lambda')\| \leq L_F \|\lambda - \lambda'\|, \quad \forall \lambda, \lambda' \in \mathbb{R}_+^N;$$

(ii) The mapping  $A : \mathbb{R}^N \rightarrow \mathbb{R}^N$  is monotone;

(iii) Weak Minty variational inequality (WMVI) holds, i.e., there exists a nonempty set  $S^* \subseteq \text{zer}T$  such that for all  $\lambda^* \in S^*$  and some  $\rho \in (-1/2L_F, +\infty)$

$$\langle v, \lambda - \lambda^* \rangle \geq \rho \|v\|^2, \quad \text{for all } (\lambda, v) \in \text{gph}T;$$

(iv) The stochastic oracle has a bounded variance:

$$\mathbb{E}_{\mathbf{H}, \xi \sim \mathcal{D}^\xi(\kappa)} \left[ \|\hat{F}(\mathbf{H}_\xi) - F(\lambda)\|^2 \right] \leq \sigma^2, \quad \forall \lambda \in \mathbb{R}_+^N;$$

**Assumption IV(i)** assumes that mapping  $F$  in (7) and (14) is Lipschitz continuous. This assumption can be readily fulfilled by taking **Assumption III** along with the structure of distribution  $\mathcal{D}^\xi$  in **Definition III.1**. The following lemma investigates this assumption.

**Lemma A.1** (sufficient conditions for **Assumption IV(i)**). *Take **Assumption III**, then **Assumption IV(i)** holds with  $L_F = \beta\omega$ , where  $\omega > 0$  is the Lipschitz constant of the distribution  $\mathcal{D}^\xi$  (cf. (15) for definition).*

*Proof:* This proof is closely following the proof in [38, lem. 2.1] and is presented here for completeness. By the Bernoulli distribution  $\mathcal{D}^\xi$  associated to USVs  $\xi$  in **Definition III.1**, and also the distribution distance measure defined in (13), the smoothness notion can be extended to the distributions. Namely, a constant  $L_{\mathcal{D}^\xi} > 0$  exists such that

$$W_1(\mathcal{D}^\xi(\kappa), \mathcal{D}^\xi(\kappa')) \leq L_{\mathcal{D}^\xi} \|\kappa - \kappa'\|. \quad (15)$$

Moreover, as in (7)  $\kappa$  is a continuous function of  $\lambda$ , a constant  $L_\kappa > 0$  exists such that

$$\|\kappa(\lambda) - \kappa(\lambda')\| \leq L_\kappa \|\lambda - \lambda'\|.$$

Hence, the composition is also Lipschitz continuous:

$$W_1(\mathcal{D}^\xi(\kappa(\lambda)), \mathcal{D}^\xi(\kappa(\lambda'))) \leq \omega \|\lambda - \lambda'\|,$$

where  $\omega := L_\kappa L_{\mathcal{D}^\xi}$  is defined.

Define  $g(\xi) := \langle v, \mathbb{E}_{\mathbf{H}} [U^{\theta^*}(\mathbf{H}_\xi)] \rangle$  with a vector  $v$  where  $\|v\| \leq 1$ . By **Assumption III**,  $g(\xi)$  is  $\beta$ -Lipschitz continuous in  $\xi$ , since:

$$\begin{aligned} \|g(\xi) - g(\xi')\| &\leq \|v\| \left\| \mathbb{E}_{\mathbf{H}} [U^{\theta^*}(\mathbf{H}_\xi)] - \mathbb{E}_{\mathbf{H}} [U^{\theta^*}(\mathbf{H}_{\xi'})] \right\| \\ &\leq \beta \|\xi - \xi'\|, \end{aligned}$$

hence:

$$\langle v, F(\lambda') - F(\lambda) \rangle = \mathbb{E}_{\xi \sim \mathcal{D}^\xi(\kappa)} [g(\xi)] - \mathbb{E}_{\xi' \sim \mathcal{D}^\xi(\kappa')} [g(\xi')]$$

$$\leq \beta W_1(\mathcal{D}^\xi(\kappa), \mathcal{D}^\xi(\kappa')),$$

where in the equality the definition of  $F$  in (7) is considered, and the inequality is due to (13) considering  $g \in \text{lip}_\beta$ . Taking  $v = F(\lambda') - F(\lambda) / \|F(\lambda') - F(\lambda)\|$  and then using (15) completes the proof with  $L_F = \beta L_\kappa L_{\mathcal{D}^\xi}$ .

It is remarked that there is no control over the constants  $\beta$  and  $L_{\mathcal{D}^\xi}$  and they are determined by the communication system and the Bernoulli distribution, respectively. However, the constant  $L_\kappa$  is adjustable by modifying  $c$  in the function  $\kappa_i = (c + \lambda_i) / \max_{\ell \in \{c + \lambda_\ell\}}$  in (7). ■

**Assumption IV(ii)** also holds because mapping  $A$  is a subdifferential of the indicator function  $\varphi$  defined in (14), hence, it is monotone. The class of nonmonotone mappings for which convergence analyses are possible is characterized by **Assumption IV(iii)**, where nonmonotonicity can be captured thanks to the possibly negative values of  $\rho$ . The mapping  $F$  defined in (7) may not be (strongly) monotone, i.e.,  $\langle v_1 - v_2, \lambda_1 - \lambda_2 \rangle \not\geq \rho \|\lambda_1 - \lambda_2\|^2$  with a  $\rho \geq 0$  for all  $(\lambda_1, v_1), (\lambda_2, v_2) \in \text{gph}T$ . This relation can be interpreted as follows: increasing  $\lambda_i$  for user  $i$  results in increasing the probability of user  $i$  being activated, which consequently increases its expected utility and decreases  $[F\lambda]_i$  due to the definition. Therefore, the relation cannot be guaranteed with a  $\rho \geq 0$ , whereas **Assumption IV(iii)**, with the possibility of  $\rho < 0$ , readily captures the relation. It is worth noting that this assumption may be considered restrictive, since  $\rho$  is lowerbounded by  $-1/2L_F$ , a value that depends on  $\omega$  and  $\beta$  according to **Lemma A.1**. Nevertheless, extensive numerical studies in **Section IV** have not witnessed divergence as long as **Assumption II** holds (cf. **Fig. 4** where **Assumption II** does not hold). Finally, **Assumption IV(iv)** is a standard assumption in stochastic optimization literature, e.g., [39], [40].

## APPENDIX B

With the necessary assumptions established and the recast problem in (14), the next theorem demonstrates the convergence of the iterations generated by **Algorithm 1**.

**Theorem B.1** (subsequential convergence). *Suppose that **Assumptions I to IV** hold. Moreover, take the step size sequence  $(\alpha_k)_{k=0}^K \in (0, 1)$  and  $\gamma > 0$ , the batchsize sequence  $(B_k)_{k=0}^K \in \mathbb{N}$ , and suppose*

$$\bar{\mu} := 2\frac{\rho}{\gamma} + \frac{1 - \sqrt{\alpha^{\max}}}{1 + \sqrt{\alpha^{\max}}} - \alpha^{\max} - 2\bar{\alpha}\gamma^2 L_F^2 \mathcal{A} > 0,$$

where  $\alpha^{\max} := \max_k \{\alpha_k\}$ ,  $\bar{\alpha} := \max_k \{\alpha_k / \alpha_{k+1}\}$ , and  $\mathcal{A} := 3 \left( \frac{1}{\sqrt{\alpha^{\max}(1-\gamma L_F)^2}} + \frac{1 - \sqrt{\alpha^{\max}}}{\sqrt{\alpha^{\max}}} \right)$ . Then, the iterates  $\bar{\lambda}^k$  generated by **Algorithm 1** hold the following estimate

$$\begin{aligned} \min_{k \in \{0, \dots, K\}} \mathbb{E} \left[ \text{dist}(\mathbf{0}, T\bar{\lambda}^k) \right] & \quad (16) \\ & \leq \frac{\|\lambda^0 - \lambda^*\|^2 + \mathcal{A} \|\mathbf{h}^{-1} - \lambda^{-1} + \gamma F \lambda^{-1}\|^2}{\gamma^2 \bar{\mu} \sum_{\ell=0}^K \alpha_\ell} \\ & \quad + \frac{\sum_{k=0}^K \{ \alpha_k^2 Q \sigma^2 / B_k + 2\alpha_k \gamma^4 L_F^2 \mathcal{A} \sigma^2 / B_k \}}{\gamma^2 \bar{\mu} \sum_{\ell=0}^K \alpha_\ell}. \end{aligned}$$

with  $Q := \gamma^2 \mathcal{A} + \gamma^2 \alpha^{\max} (\mathcal{A}/3 + \gamma^2)$ .

*Proof: Define the following operators:*

$$H := \text{id} - \gamma F, \quad \bar{H} := \text{id} - \gamma \hat{F}(\mathbb{H}_{\xi}^k), \quad (17)$$

and the filtration:

$$\mathcal{F}_k := \text{filtration}\{\mathbb{H}_{\xi}^0, \bar{\mathbb{H}}_{\xi}^0, \dots, \mathbb{H}_{\xi}^{k-1}, \bar{\mathbb{H}}_{\xi}^{k-1}\},$$

where includes all the randomness involved up to iteration  $k$ . Take the Lyapunov function:

$$\begin{aligned} \mathcal{U}_{k+1} &:= \left\| \boldsymbol{\lambda}^{k+1} - \boldsymbol{\lambda}^* \right\|^2 \\ &\quad + \mathcal{A}_{k+1} \left\| \mathbf{h}^k - H\boldsymbol{\lambda}^k \right\|^2 + \mathcal{B}_{k+1} \left\| \boldsymbol{\lambda}^{k+1} - \boldsymbol{\lambda}^k \right\|^2. \end{aligned} \quad (18)$$

Expanding the first term results in,

$$\begin{aligned} \left\| \boldsymbol{\lambda}^{k+1} - \boldsymbol{\lambda}^* \right\|^2 &= \left\| \boldsymbol{\lambda}^k - \boldsymbol{\lambda}^* \right\|^2 \\ &\quad - 2\alpha_k \langle \mathbf{h}^k - \bar{H}\bar{\boldsymbol{\lambda}}^k, \boldsymbol{\lambda}^k - \boldsymbol{\lambda}^* \rangle + \alpha_k^2 \left\| \mathbf{h}^k - \bar{H}\bar{\boldsymbol{\lambda}}^k \right\|^2. \end{aligned} \quad (19)$$

We continue by upperbounding the terms in (18) and (19). The term  $\left\| \mathbf{h}^k - H\boldsymbol{\lambda}^k \right\|^2$  is upperbounded as follows:

$$\begin{aligned} \mathbf{h}^k - H\boldsymbol{\lambda}^k &= \gamma F\boldsymbol{\lambda}^k - \gamma \hat{F}(\mathbb{H}_{\xi}^k) + (1 - \alpha_k) \left( \mathbf{h}^{k-1} - \boldsymbol{\lambda}^{k-1} + \gamma \hat{F}(\mathbb{H}_{\xi}^k) \right), \\ \left\| \mathbf{h}^k - H\boldsymbol{\lambda}^k \right\|^2 &= (1 - \alpha_k)^2 \left\| \mathbf{h}^{k-1} - \boldsymbol{\lambda}^{k-1} + \gamma F\boldsymbol{\lambda}^k \right\|^2 \\ &\quad + \left\| \gamma F\boldsymbol{\lambda}^k - \gamma \hat{F}(\mathbb{H}_{\xi}^k) + (1 - \alpha_k) \left( \gamma \hat{F}(\mathbb{H}_{\xi}^k) - \gamma F\boldsymbol{\lambda}^k \right) \right\|^2 \\ &\quad + 2(1 - \alpha_k) \langle \mathbf{h}^{k-1} - \boldsymbol{\lambda}^{k-1} + \gamma F\boldsymbol{\lambda}^k, \\ &\quad \gamma F\boldsymbol{\lambda}^k - \gamma \hat{F}(\mathbb{H}_{\xi}^k) + (1 - \alpha_k) (\gamma \hat{F}(\mathbb{H}_{\xi}^k) - \gamma F\boldsymbol{\lambda}^k) \rangle, \end{aligned} \quad (20)$$

where the first equality is due to the definition of  $H$  in (17) and  $\mathbf{h}^k$  in Algorithm 1. The second equality is also derived by adding and subtracting  $(1 - \alpha_k)\gamma F\boldsymbol{\lambda}^k$ . By taking the expectation conditioned on  $\mathcal{F}_k$ , the first term in the vector inner product is deterministic, while the second term vanishes due to unbiasedness of  $\hat{F}$  in (6) and (8). Hence, the last term is zero in expectation. Hence,

$$\begin{aligned} \mathbb{E} \left[ \left\| \mathbf{h}^k - H\boldsymbol{\lambda}^k \right\|^2 \mid \mathcal{F}_k \right] &= (1 - \alpha_k)^2 \left\| \mathbf{h}^{k-1} - \boldsymbol{\lambda}^{k-1} + \gamma F\boldsymbol{\lambda}^k \right\|^2 \\ &\quad + \alpha_k^2 \gamma^2 \mathbb{E} \left[ \left\| \hat{F}(\mathbb{H}_{\xi}^k) - F\boldsymbol{\lambda}^k \right\|^2 \mid \mathcal{F}_k \right] \\ &\leq (1 + e_k)(1 - \alpha_k)^2 \left\| \mathbf{h}^{k-1} - \boldsymbol{\lambda}^{k-1} + \gamma F\boldsymbol{\lambda}^{k-1} \right\|^2 \\ &\quad + (1 + 1/e_k)(1 - \alpha_k)^2 \left\| \gamma F\boldsymbol{\lambda}^k - \gamma F\boldsymbol{\lambda}^{k-1} \right\|^2 + \gamma^2 \alpha_k^2 \sigma_k^2 \\ &\leq U_1 \left\| \mathbf{h}^{k-1} - \boldsymbol{\lambda}^{k-1} + \gamma F\boldsymbol{\lambda}^{k-1} \right\|^2 + U_2 \left\| \boldsymbol{\lambda}^k - \boldsymbol{\lambda}^{k-1} \right\|^2 + U_3 \end{aligned} \quad (21)$$

with

$$U_1^k := (1 + e_k)(1 - \alpha_k)^2, \quad U_2^k := (1 + 1/e_k)(1 - \alpha_k)^2 L_F^2 \gamma^2, \\ U_3^k := \gamma^2 \alpha_k^2 \sigma_k^2, \quad \text{and } \sigma_k^2 := \sigma^2 / B_k,$$

where the first inequality is derived by adding and subtracting  $\gamma F\boldsymbol{\lambda}^{k-1}$  along with the Young's inequality with a sequence of  $e_k > 0$ . In addition, Assumption IV(iv) is invoked for a minibatch of size  $B_k$  to have

$$\mathbb{E} \left[ \left\| \hat{F}(\mathbb{H}_{\xi}^k) - F\boldsymbol{\lambda}^k \right\|^2 \mid \mathcal{F}_k \right] \quad (22)$$

$$= \mathbb{E} \left[ \left\| \frac{1}{B_k} \sum_{j=1}^{B_k} \hat{F}(\mathbf{H}_{\xi}^j) - F\boldsymbol{\lambda}^k \right\|^2 \mid \mathcal{F}_k \right] \leq \sigma^2 / B_k.$$

To bound the last term in (19),

$$\begin{aligned} \alpha_k^2 \mathbb{E} \left[ \left\| \mathbf{h}^k - \bar{H}\bar{\boldsymbol{\lambda}}^k \right\|^2 \mid \mathcal{F}_k \right] &= \alpha_k^2 \left\| \mathbf{h}^k - H\bar{\boldsymbol{\lambda}}^k \right\|^2 + \alpha_k^2 \gamma^2 \mathbb{E} \left[ \left\| F\bar{\boldsymbol{\lambda}}^k - \hat{F}(\bar{\mathbb{H}}_{\xi}^k) \right\|^2 \mid \mathcal{F}_k \right] \\ &\leq \alpha_k^2 \left\| \mathbf{h}^k - H\bar{\boldsymbol{\lambda}}^k \right\|^2 + \alpha_k^2 \gamma^2 \sigma_k^2, \end{aligned} \quad (23)$$

where the first equality is by adding and subtracting  $\gamma F\bar{\boldsymbol{\lambda}}^k$  and the fact that  $\hat{F}$  is unbiased due to (6) and (8). The last inequality is also due to Assumption IV(iv).

Similarly, the last term in (18) can be bounded by

$$\begin{aligned} \mathbb{E} \left[ \left\| \boldsymbol{\lambda}^{k+1} - \boldsymbol{\lambda}^k \right\|^2 \mid \mathcal{F}_k \right] &= \alpha_k^2 \mathbb{E} \left[ \left\| \mathbf{h}^k - \bar{H}\bar{\boldsymbol{\lambda}}^k \right\|^2 \mid \mathcal{F}_k \right] \\ &\leq \alpha_k^2 \left\| \mathbf{h}^k - H\bar{\boldsymbol{\lambda}}^k \right\|^2 + \alpha_k^2 \gamma^2 \sigma_k^2, \end{aligned} \quad (24)$$

due to step 7 of Algorithm 1 and (23).

To bound the second term in the rhs of (19), we refer to the following lemma:

**Lemma B.2** (bounding of  $-2\alpha_k \langle \mathbf{h}^k - \bar{H}\bar{\boldsymbol{\lambda}}^k, \boldsymbol{\lambda}^k - \boldsymbol{\lambda}^* \rangle$ ). Take assumptions Assumptions IV(i) to IV(iii). Then the following bound holds:

$$\begin{aligned} -2\alpha_k \mathbb{E} \left[ \langle \mathbf{h}^k - \bar{H}\bar{\boldsymbol{\lambda}}^k, \boldsymbol{\lambda}^k - \boldsymbol{\lambda}^* \rangle \mid \mathcal{F}_k \right] &\leq \alpha(\epsilon_1 + \frac{1}{\epsilon_2} \Delta) \mathbb{E} \left[ \left\| \mathbf{h}^k - H\boldsymbol{\lambda}^k \right\|^2 \mid \mathcal{F}_k \right] \\ &\quad - \left( \frac{\alpha_k}{1 + \epsilon_2} \Delta + 2\alpha_k \frac{\rho}{\gamma} \right) \mathbb{E} \left[ \left\| \mathbf{h}^k - H\bar{\boldsymbol{\lambda}}^k \right\|^2 \mid \mathcal{F}_k \right], \end{aligned}$$

with  $\Delta := 1 - \frac{1}{\epsilon_1(1 - \gamma L_F)^2} \geq 0$ , and some positive  $\epsilon_1$  and  $\epsilon_2$ .

Define the following

$$\begin{aligned} \mu_k &:= 2\frac{\rho}{\gamma} + \frac{\Delta}{1 + \epsilon_2} - \alpha_k(1 + \mathcal{B}_{k+1}) \\ X_1^k &:= \mathcal{A}_{k+1} + \epsilon_1 \alpha_k + \frac{\Delta}{\epsilon_2} \alpha_k \\ X_2^k &:= \alpha_k^2 \gamma^2 \sigma_k^2 (1 + \mathcal{B}_{k+1}). \end{aligned} \quad (25)$$

Putting bounds derived in (23), (24), and Lemma B.2 into the Lyapunov function (18) results in

$$\begin{aligned} \mathbb{E}[\mathcal{U}_{k+1} \mid \mathcal{F}_k] &\leq \left\| \boldsymbol{\lambda}^k - \boldsymbol{\lambda}^* \right\|^2 - \alpha_k \mu_k \mathbb{E} \left[ \left\| \mathbf{h}^k - H\bar{\boldsymbol{\lambda}}^k \right\|^2 \mid \mathcal{F}_k \right] \\ &\quad + X_1^k \mathbb{E} \left[ \left\| \mathbf{h}^k - H\boldsymbol{\lambda}^k \right\|^2 \mid \mathcal{F}_k \right] + X_2^k. \end{aligned} \quad (26)$$

Considering the bound for  $\left\| \mathbf{h}^k - H\boldsymbol{\lambda}^k \right\|^2$  derived in (21), the following is concluded:

$$\begin{aligned} \mathbb{E}[\mathcal{U}_{k+1} \mid \mathcal{F}_k] - \mathcal{U}_k &\leq -\alpha_k \mu_k \mathbb{E} \left[ \left\| \mathbf{h}^k - H\bar{\boldsymbol{\lambda}}^k \right\|^2 \mid \mathcal{F}_k \right] \\ &\quad + (U_1^k X_1^k - \mathcal{A}_k) \left\| \mathbf{h}^{k-1} - H\boldsymbol{\lambda}^{k-1} \right\|^2 \\ &\quad + (U_2^k X_1^k - \mathcal{B}_k) \left\| \boldsymbol{\lambda}^k - \boldsymbol{\lambda}^{k-1} \right\|^2 \\ &\quad + U_3^k X_1^k + X_2^k. \end{aligned} \quad (27)$$

with  $U_1^k, U_2^k$  and  $U_3^k$  defined in (21). To guarantee descent in (27), we need to satisfy the bounds  $\epsilon_1 > 0, \epsilon_2 > 0$ , and  $\Delta \geq 0$  defined in Lemma B.2, along with  $\mu_k > 0, U_1^k X_1^k - \mathcal{A}_k \leq 0$ ,



and  $U_2^k X_1^k - \mathcal{B}_k \leq 0$ . Hence, with  $\alpha^{\max} := \max_k \{\alpha_k\}$ , the parameters are set as follows:

- $\Delta \geq 0 \implies \epsilon_1 \geq 1/(1-\gamma L_F)^2$ , set:  $\epsilon_1 = 1/\sqrt{\alpha^{\max}(1-\gamma L_F)^2}$
- $U_1^k X_1^k - \mathcal{A}_k \leq 0 \implies$  take:  $A_k = \mathcal{A} \implies$   
 $(1-\alpha_k)^2(1+e_k)\mathcal{A} + (1-\alpha_k)^2(1+e_k)\alpha_k(\epsilon_1 + \frac{\Delta}{\epsilon_2}) - \mathcal{A}$   
 $\leq -\alpha_k\mathcal{A} + e_k(1-\alpha_k)\mathcal{A} + (1-\alpha_k)^2(1+e_k)\alpha_k(\epsilon_1 + \frac{\Delta}{\epsilon_2})$   
 $\leq -\alpha_k(1 - e_k/\alpha_k)\mathcal{A} + (1+e_k)\alpha_k(\epsilon_1 + \frac{\Delta}{\epsilon_2}) \leq 0$   
 $\implies \mathcal{A} \geq \frac{(1+\nu)(\epsilon_1 + \Delta/\epsilon_2)}{1-\nu}$ , with  $\nu := e_k/\alpha_k \in (0, 1)$ ,  
 set:  $\epsilon_2 = \sqrt{\alpha^{\max}} \implies \Delta = 1 - \sqrt{\alpha^{\max}}$  and  
 $\mathcal{A} = \frac{1+\nu}{1-\nu} \left( \frac{1}{\sqrt{\alpha^{\max}(1-\gamma L_F)^2}} + \frac{1-\sqrt{\alpha^{\max}}}{\sqrt{\alpha^{\max}}} \right)$
- $U_2^k X_1^k - \mathcal{B}_k \leq 0 \implies$  take:  $\mathcal{B}_k = \frac{U_2^k}{U_1^k} \mathcal{A} = \frac{1}{e_k} \gamma^2 L_F^2 \mathcal{A}$
- $\mu_k > 0 \implies 2\frac{\rho}{\gamma} + \frac{\Delta}{1+\epsilon_2} - \alpha_k(1+\mathcal{B}_{k+1})$  (28)  
 $= 2\frac{\rho}{\gamma} + \frac{\Delta}{1+\epsilon_2} - \alpha_k - \frac{\alpha_k}{e_{k+1}} \gamma^2 L_F^2 \mathcal{A}$   
 $\geq 2\frac{\rho}{\gamma} + \frac{1-\sqrt{\alpha^{\max}}}{1+\sqrt{\alpha^{\max}}} - \alpha^{\max} - \frac{\bar{\alpha}}{\nu} \gamma^2 L_F^2 \mathcal{A} =: \bar{\mu} \geq 0$   
 with  $\bar{\alpha} := \max_k \{\alpha_k/\alpha_{k+1}\}$ ,

where in the first bullet,  $\epsilon_1$  is chosen due to  $\alpha^{\max} \in (0, 1)$ . In the second bullet, the first inequality is due to  $(1-\alpha_k)^2 < 1-\alpha_k$ , and the second inequality is due to  $(1-\alpha_k)^2 < 1$ , and  $(1-\alpha_k) < 1$ . The third bullet uses the relation of  $U_2^k X_1^k - \mathcal{B}_k$  with  $U_1^k X_1^k - \mathcal{A}_k$ . In the last bullet,  $\alpha^{\max} \geq \alpha_k$  is considered due to the diminishing step size assumption. The last term in (27) can also be upperbounded as

$$U_3^k X_1^k + X_2^k \leq \alpha_k^2 \sigma_k^2 Q + \alpha_k \sigma_k^2 \gamma^4 L_F^2 \mathcal{A} / \nu,$$

where  $Q := \gamma^2 \mathcal{A} + \gamma^2 \alpha^{\max} (\epsilon_1 + \Delta/\epsilon_2 + \gamma^2)$ ,  $\alpha^{\max} \geq \alpha_k$  and the definition of  $\nu$  is considered. Putting the above inequalities back into (27) results in

$$\mathbb{E}[U_{k+1} | \mathcal{F}_k] - U_k \leq -\alpha_k \mu_k \mathbb{E} \left[ \left\| \mathbf{h}^k - H \bar{\lambda}^k \right\|^2 | \mathcal{F}_k \right] + \alpha_k^2 \sigma_k^2 Q + \alpha_k \sigma_k^2 \gamma^4 L_F^2 \mathcal{A} / \nu. \quad (29)$$

Taking the total expectation, rearranging, and telescoping results in

$$\bar{\mu} \sum_{k=0}^K \alpha_k \mathbb{E} \left[ \left\| \mathbf{h}^k - H \bar{\lambda}^k \right\|^2 \right] \leq \mathcal{U}_0 - \mathbb{E}[U_{K+1}] + \sum_{k=0}^K \{ \alpha_k^2 \sigma_k^2 Q + \alpha_k \sigma_k^2 \gamma^4 L_F^2 \mathcal{A} / \nu \}$$

where  $\bar{\mu}$  is defined in (28). Omitting  $\mathbb{E}[U_{K+1}] > 0$  from rhs and dividing both sides by  $\bar{\mu} \sum_{k=0}^K \alpha_k$  gives

$$\sum_{k=0}^K \frac{\alpha_k}{\sum_{\ell=0}^K \alpha_\ell} \mathbb{E} \left[ \left\| \mathbf{h}^k - H \bar{\lambda}^k \right\|^2 \right] \leq \frac{\left\| \lambda^0 - \lambda^* \right\|^2 + \mathcal{A} \left\| \mathbf{h}^{-1} - \lambda^{-1} + \gamma F \lambda^{-1} \right\|^2}{\bar{\mu} \sum_{\ell=0}^K \alpha_\ell} + \frac{\sum_{k=0}^K \{ \alpha_k^2 \sigma_k^2 Q + \alpha_k \sigma_k^2 \gamma^4 L_F^2 \mathcal{A} / \nu \}}{\bar{\mu} \sum_{\ell=0}^K \alpha_\ell}. \quad (30)$$

Moreover,

$$\left\| \mathbf{h}^k - H \bar{\lambda}^k \right\|^2 = \left\| \gamma T \bar{\lambda}^k \right\|^2 \geq \text{dist}(\mathbf{0}, \gamma T \bar{\lambda}^k),$$

where  $\mathbf{h}^k \in \bar{\lambda}^k + \gamma A \bar{\lambda}^k$  is used due to [step 4 of Algorithm 1](#), as the step imposes the update  $\bar{\lambda}^k = (\text{id} + \gamma A)^{-1} \mathbf{h}^k = \max\{\mathbf{0}, \mathbf{h}^k\}$ . The lhs of (30) can also be lowerbounded by the  $\min\{\cdot\}$  operator as it is a weighted sum. Hence,

$$\min_{k \in \{0, \dots, K\}} \mathbb{E} \left[ \text{dist}(\mathbf{0}, T \bar{\lambda}^k) \right] \leq \frac{\left\| \lambda^0 - \lambda^* \right\|^2 + \mathcal{A} \left\| \mathbf{h}^{-1} - \lambda^{-1} + \gamma F \lambda^{-1} \right\|^2}{\gamma^2 \bar{\mu} \sum_{\ell=0}^K \alpha_\ell} + \frac{\sum_{k=0}^K \{ \alpha_k^2 \sigma_k^2 Q + \alpha_k \sigma_k^2 \gamma^4 L_F^2 \mathcal{A} / \nu \}}{\gamma^2 \bar{\mu} \sum_{\ell=0}^K \alpha_\ell}.$$

Setting  $\nu = 0.5$ , and using (22) completes the proof.  $\blacksquare$

The same estimate for  $\mathbb{E} \left[ \text{dist}(\mathbf{0}, T \bar{\lambda}^k) \right]$ —indicating  $\mathbf{0} \in T \bar{\lambda}^k$  in (14) if  $\text{dist}(\mathbf{0}, T \bar{\lambda}^k) = 0$ —is presented in [39], except for the last term on the rhs. This difference is due to the independence of the stochastic oracle  $\hat{F}$  from the decision variable  $\lambda$ . Moreover, the condition type on  $\bar{\mu}$  can also be found in [39], where it can be controlled by adjusting  $\alpha^{\max}$  as well as  $L_F$ . It should be mentioned that the Lipschitz constant  $L_F$  can be chosen arbitrarily small (cf. [Lemma A.1](#)).

The estimate in (16) indicates the possibility of achieving a diminishing rhs, and consequently, convergence to a fixed point, by selecting suitable step sizes  $\alpha_k$  and batch sizes  $B_k$ . The following remark highlights the convergence rate achieved through the standard choice of these parameters [40]:

**Remark B.3.** Consider the following two scenarios:

- Take fixed step size  $\alpha_k = \alpha$  and fixed batchsize  $B_k = \sqrt{K}$ ;
- Take diminishing step size  $\alpha_k = \frac{\alpha_0}{\sqrt{1+\alpha k}}$  and the increasing batchsize  $B_k = 1 + \sqrt{k}$ , with some positive  $\alpha_0$  and  $\tilde{\alpha}$ .

Then, in both scenarios, the convergence rate is

$$\min_{k \in \{0, \dots, K\}} \mathbb{E} \left[ \text{dist}(\mathbf{0}, T \bar{\lambda}^k) \right] \leq \mathcal{O}(1/\sqrt{K}).$$

$\square$

## REFERENCES

- [1] V. P. Mhatre, K. Papagiannaki, and F. Baccelli, “Interference mitigation through power control in high density 802.11 WLANs,” in *INFOCOM 26th IEEE International Conference on Computer Communications*, 2007, pp. 535–543.
- [2] R. Cendrillon, J. Huang, M. Chiang, and M. Moonen, “Autonomous spectrum balancing for digital subscriber lines,” *IEEE Transactions on Signal Processing*, vol. 55, no. 8, pp. 4241–4257, 2007.
- [3] M. Chiang, C. W. Tan, D. P. Palomar, D. O’neill, and D. Julian, “Power control by geometric programming,” *IEEE transactions on wireless communications*, vol. 6, no. 7, pp. 2640–2651, 2007.
- [4] Q. Shi, M. Razaviyayn, Z.-Q. Luo, and C. He, “An Iteratively Weighted MMSE Approach to Distributed Sum-Utility Maximization for a MIMO Interfering Broadcast Channel,” *IEEE Transactions on Signal Processing*, vol. 59, no. 9, pp. 4331–4340, 2011.

- [5] F. Zhou, G. Lu, M. Wen, Y.-C. Liang, Z. Chu, and Y. Wang, "Dynamic spectrum management via machine learning: State of the art, taxonomy, challenges, and open research issues," *IEEE Network*, vol. 33, no. 4, pp. 54–62, 2019.
- [6] W. Tong and G. Y. Li, "Nine Challenges in Artificial Intelligence and Wireless Communications for 6G," *IEEE Wireless Communications*, pp. 1–10, 2022.
- [7] H. Sun, X. Chen, Q. Shi, M. Hong, X. Fu, and N. D. Sidiropoulos, "Learning to optimize: Training deep neural networks for interference management," *IEEE Transactions on Signal Processing*, vol. 66, no. 20, pp. 5438–5453, 2018.
- [8] F. Liang, C. Shen, W. Yu, and F. Wu, "Towards Optimal Power Control via Ensembling Deep Neural Networks," *IEEE Transactions on Communications*, vol. 68, no. 3, pp. 1760–1776, 2020.
- [9] W. Lee, "Resource allocation for multi-channel underlay cognitive radio network based on deep neural network," *IEEE Communications Letters*, vol. 22, no. 9, pp. 1942–1945, 2018.
- [10] L. Liang, H. Ye, G. Yu, and G. Y. Li, "Deep-Learning-Based Wireless Resource Allocation With Application to Vehicular Networks," *Proceedings of the IEEE*, vol. 108, no. 2, pp. 341–356, 2020.
- [11] W. Cui, K. Shen, and W. Yu, "Spatial Deep Learning for Wireless Scheduling," *IEEE Journal on Selected Areas in Communications*, vol. 37, no. 6, pp. 1248–1261, 2019.
- [12] L. Liang, H. Ye, and G. Y. Li, "Spectrum sharing in vehicular networks based on multi-agent reinforcement learning," *IEEE Journal on Selected Areas in Communications*, vol. 37, no. 10, pp. 2282–2292, 2019.
- [13] H. Ye, G. Y. Li, and B.-H. F. Juang, "Deep Reinforcement Learning Based Resource Allocation for V2V Communications," *IEEE Transactions on Vehicular Technology*, vol. 68, no. 4, pp. 3163–3173, 2019.
- [14] C. Guo, Z. Li, L. Liang, and G. Y. Li, "Reinforcement Learning Based Power Control for Reliable Wireless Transmission," *arXiv preprint arXiv:2202.06345*, 2022.
- [15] Y. S. Nasir and D. Guo, "Multi-Agent Deep Reinforcement Learning for Dynamic Power Allocation in Wireless Networks," *IEEE Journal on Selected Areas in Communications*, vol. 37, no. 10, pp. 2239–2250, 2019.
- [16] R. S. Sutton, D. McAllester, S. Singh, and Y. Mansour, "Policy gradient methods for reinforcement learning with function approximation," *Advances in neural information processing systems*, vol. 12, 1999.
- [17] M. Eisen, C. Zhang, L. F. O. Chamon, D. D. Lee, and A. Ribeiro, "Learning Optimal Resource Allocations in Wireless Systems," *IEEE Transactions on Signal Processing*, vol. 67, no. 10, pp. 2775–2790, 2019.
- [18] D. S. Kalogerias, M. Eisen, G. J. Pappas, and A. Ribeiro, "Model-Free Learning of Optimal Ergodic Policies in Wireless Systems," *IEEE Transactions on Signal Processing*, vol. 68, pp. 6272–6286, 2020.
- [19] Z. Wang, M. Eisen, and A. Ribeiro, "Learning Decentralized Wireless Resource Allocations With Graph Neural Networks," *IEEE Transactions on Signal Processing*, vol. 70, pp. 1850–1863, 2022.
- [20] Z. Wu, S. Pan, F. Chen, G. Long, C. Zhang, and P. S. Yu, "A Comprehensive Survey on Graph Neural Networks," *IEEE Transactions on Neural Networks and Learning Systems*, vol. 32, no. 1, pp. 4–24, 2021.
- [21] Y. Shen, Y. Shi, J. Zhang, and K. B. Letaief, "Graph Neural Networks for Scalable Radio Resource Management: Architecture Design and Theoretical Analysis," *IEEE Journal on Selected Areas in Communications*, vol. 39, no. 1, pp. 101–115, 2021.
- [22] N. NaderiAlizadeh, M. Eisen, and A. Ribeiro, "Learning resilient radio resource management policies with graph neural networks," *IEEE Transactions on Signal Processing*, vol. 71, pp. 995–1009, 2023.
- [23] M. Eisen and A. Ribeiro, "Optimal Wireless Resource Allocation With Random Edge Graph Neural Networks," *IEEE Transactions on Signal Processing*, vol. 68, pp. 2977–2991, 2020.
- [24] N. NaderiAlizadeh, M. Eisen, and A. Ribeiro, "State-augmented learnable algorithms for resource management in wireless networks," *IEEE Transactions on Signal Processing*, vol. 70, pp. 5898–5912, 2022.
- [25] P. Behmandpoor, P. Patrinos, and M. Moonen, "Federated learning based resource allocation for wireless communication networks," in *30th European Signal Processing Conference (EUSIPCO)*, 2022, pp. 1656–1660.
- [26] —, "Model-free decentralized training for deep learning based resource allocation in communication networks," in *31st European Signal Processing Conference (EUSIPCO)*, 2023, pp. 1494–1498.
- [27] P. Behmandpoor, J. Verdyck, and M. Moonen, "Deep learning-based cross-layer resource allocation for wired communication systems," in *ICASSP International Conference on Acoustics, Speech and Signal Processing*. IEEE, 2021, pp. 4120–4124.
- [28] R. Dong, C. She, W. Hardjawana, Y. Li, and B. Vucetic, "Deep Learning for Radio Resource Allocation With Diverse Quality-of-Service Requirements in 5G," *IEEE Transactions on Wireless Communications*, vol. 20, no. 4, pp. 2309–2324, 2021.
- [29] S. J. Pan and Q. Yang, "A Survey on Transfer Learning," *IEEE Transactions on Knowledge and Data Engineering*, vol. 22, no. 10, pp. 1345–1359, 2010.
- [30] A. Vettoruzzo, M.-R. Bouguelia, J. Vanschoren, T. Rognvaldsson, and K. Santosh, "Advances and challenges in meta-learning: A technical review," *IEEE Trans. on Pattern Analysis and Machine Intelligence*, 2024.
- [31] A. Nagabandi, I. Clavera, S. Liu, R. S. Fearing, P. Abbeel, S. Levine, and C. Finn, "Learning to adapt in dynamic, real-world environments through meta-reinforcement learning," *preprint arXiv:1803.11347*, 2018.
- [32] C. Finn, P. Abbeel, and S. Levine, "Model-agnostic meta-learning for fast adaptation of deep networks," in *International conference on machine learning*. PMLR, 2017, pp. 1126–1135.
- [33] K. Li and J. Malik, "Learning to optimize," *arXiv preprint arXiv:1606.01885*, 2016.
- [34] P. Behmandpoor, P. Patrinos, and M. Moonen, "Learning-based resource allocation with dynamic data rate constraints," in *ICASSP International Conference on Acoustics, Speech and Signal Processing*. IEEE, 2022, pp. 4088–4092.
- [35] Y.-G. Hsieh, F. Iutzeler, J. Malick, and P. Mertikopoulos, "Explore aggressively, update conservatively: Stochastic extragradient methods with variable stepsize scaling," *Advances in Neural Information Processing Systems*, vol. 33, pp. 16 223–16 234, 2020.
- [36] J. Diakonikolas, C. Daskalakis, and M. I. Jordan, "Efficient methods for structured nonconvex-nonconcave min-max optimization," in *International Conference on Artificial Intelligence and Statistics*. PMLR, 2021, pp. 2746–2754.
- [37] L. P. Qian, Y. J. Zhang, and J. Huang, "MAPEL: Achieving global optimality for a non-convex wireless power control problem," *IEEE Transactions on Wireless Communications*, vol. 8, no. 3, pp. 1553–1563, 2009.
- [38] D. Drusvyatskiy and L. Xiao, "Stochastic optimization with decision-dependent distributions," *Mathematics of Operations Research*, vol. 48, no. 2, pp. 954–998, 2023.
- [39] T. Pethick, O. Fercoq, P. Latafat, P. Patrinos, and V. Cevher, "Solving stochastic weak minty variational inequalities without increasing batch size," *arXiv preprint arXiv:2302.09029*, 2023.
- [40] S. Ghadimi, G. Lan, and H. Zhang, "Mini-batch stochastic approximation methods for nonconvex stochastic composite optimization," *Mathematical Programming*, vol. 155, no. 1, pp. 267–305, 2016.